# Energy conservation by collective movement in schooling fish

Yangfan Zhang[1]*, George V. Lauder[1],

[1]Department of Organismic and Evolutionary Biology, Harvard University, 26 Oxford St, Cambridge, Massachusetts, 02138, USA

*Corresponding author. Email: yangfan_zhang@fas.harvard.edu

**Short title:** Energy conservation by schooling fish

**Abstract**

Many animals moving through fluids exhibit highly coordinated group movement that is thought to reduce the cost of locomotion. However, direct energetic measurements demonstrating the energy-saving benefits of fluid-mediated collective movements remain elusive. By characterizing both aerobic and anaerobic metabolic energy contributions in schools of giant danio (*Devario aequipinnatus*), we discovered that fish schools have a concave upward shaped metabolism–speed curve, with a minimum metabolic cost at ~1 body length $s^{-1}$. We demonstrate that fish schools reduce total energy expenditure (TEE) per tail beat by up to 56% compared to solitary fish. When reaching their maximum sustained swimming speed, fish swimming in schools had a 44% higher maximum aerobic performance and used 65% less non-aerobic energy compared to solitary individuals, which lowered the TEE and total cost of transport by up to 53%, near the lowest recorded for any aquatic organism. Fish in schools also recovered from exercise 43% faster than solitary fish. The non-aerobic energetic savings that occur when fish in schools actively swim at high speed can considerably improve both peak and repeated performance which is likely to be beneficial for evading predators. These energetic savings may underlie the prevalence of coordinated group locomotion in fishes.

**One-Sentence Summary:** Fish schools showed a *U*-shaped metabolism-speed curve and reduced the energy use per tail beat up to 56% at high swimming speeds compared to solitary fish.

## Introduction

Newton's laws of motion underpin animal locomotion, from fine-scale maneuvers to long-distance migrations (*1*). As speed increases or during migration involving sustained movement over long distances, animals often move in coordinated groups: *e.g.*, migratory birds in V-formation (*2*), ducklings swimming in formation (*3*), cyclists in a peloton (*4*), elite marathon runners (*5*), and fish schools (*6*). To overcome gravitational or fluid dynamic resistance to forward motion, animals use both aerobic and glycolytic metabolism (oxidative and substrate-level phosphorylation at the cellular level) to generate energy and sustain movement in the air, on land, and in the water. In water, a fluid that is 50 times more viscous than air and contains much less $O_2$ per Kg than air, the need for aquatic animals to reduce fluid dynamic drag for energy conservation is even greater than for aerial or terrestrial locomotion. Hence, we use fish schooling behaviour as a model system to explore whether the fluid dynamics of collective movement (active and directional movement of animal groups along a common trajectory (*7*)) can enable energetic savings compared to locomotion by a solitary individual. Fish schooling behaviours are some of the most prominent social and group activities exhibited by vertebrates.

Fish may school for many reasons, including foraging, reproduction, and migration, and fish schools often exhibit high-speed movement during evasion from predators. Hence, natural selection can put pressure on the formation of schools and individual interactions within a school. Besides 'safety in numbers' where individuals in a large school have a lower probability of becoming prey, can there be more tangible energetic benefits of high-speed swimming as a school? Since fluid drag scales as velocity squared (*8*), movement at higher speeds places a premium on mechanisms to conserve energy. Fast and unsustainable swimming is fueled by aerobic metabolism with a major contribution from anaerobic glycolysis (*9*) (*10*). During high-speed swimming aerobic capacity is maximized (*10*), and energy use is more likely to compete

with other activities than in low-speed swimming which only occupies a small portion of aerobic capacity. The direct consequences of unsustainably engaging anaerobic glycolysis include both fatigue and metabolic perturbation (such as changing blood acidity) that need time to recover after bouts of intense locomotion. Animals become vulnerable during recovery because of their hindered ability to repeat peak locomotor performance in the presence of predators.

Another factor of importance in the experimental evaluation of the energetic cost of collective locomotion in fishes is that endurance and efficiency are often key to achieving lifetime fitness, especially in fish species that undergo significant migrations. Fish groups usually undergo long-distance migrations at slow speeds ranging from 0.25–1.0 BL $s^{-1}$ as recorded by tags on migrating fish (Fig. S1). The common migratory speed of ~1 BL $s^{-1}$ for marine and anadromous fish could be related to the minimum aerobic cost of transport (*11*). However, there is currently no direct measurement of the absolute cost of teleost fish locomotion demonstrating a minimum group metabolic rate ($\dot{M}O_2$) at an optimal speed ($U_{opt}$). Fish schools in nature swim over a wide range of speeds (Fig. S1) but no study has directly characterized the total energy expenditure (TEE), and accounted for the potentially substantial anaerobic metabolic costs involved in higher speed locomotion. As a result, the swimming TEE performance curve of fish schools from the minimum swimming speed to the critical swimming speed ($U_{crit}$) has not yet been measured.

More broadly, despite the widespread notion that collective motion saves energy (*6*), very few studies have directly measured the energetic cost of collective movement compared to the cost of movement by solitary individuals. In the canonical case of V-formation flight in birds, energetic saving is exclusively inferred from indirect measurements, *e.g.,* heart rate (*2*), and flapping frequency and phase (*12*) (Table 1). There are no direct measurements of metabolic energy consumption of collective movement in birds, and indeed this would be extremely

challenging to accomplish. Although some energetic aspects of schooling fishes have been studied (*13*) (*14*) (*15*) (*16*) (*17*), these studies have analyzed a limited range of speeds and focused on aerobic metabolism (*see* Table 1). In fact, several field and laboratory kinematic studies suggest that both bird flocks and fish schools do not always conserve aerobic energy (*17*) (*18*) (*19*) and indicate that moving in a group can actually involve *increased* costs. Without directly measuring the energetic cost of movement, inferences solely based on kinematics do not include complex group interactions, and the interaction between collective behaviour and fluid dynamics. Consequently, we do not yet have a holistic and mechanistic view of where and how the collective movement by fish might conserve energy.

For swimming fish, fluid dynamic experiments have shown how collective movement can improve swimming efficiency due to interactions among deforming bodies and through interactions between moving animals and the local fluid environment (these energy-saving mechanisms are summarized in Fig. 1). Our current understanding of energy saving mechanisms during collective locomotion in fishes is largely based on computational fluid dynamic models with a few analyses using robotic systems (*6*) (*20*) (*21*) (*22*) (*23*) at low speed, but the link between such models and fish metabolic energy saving over a wide speed range is not yet established. We expect that the need to conserve energy in animals moving against air or water resistance should be greater at higher speeds. We hypothesize that fish in schools can reduce the total cost of high-speed locomotion relative to solitary movement, leading to reduced non-aerobic energetic costs and time of recovery for schooling fish swimming at speeds occupying the majority (> 50%) of their aerobic capacity. Our secondary objective is to determine the differences (if any) between the swimming performance curves (metabolism versus speed) of solitary fish and fish schools.

To evaluate these hypotheses, we directly measured both the aerobic and non-aerobic energy used by schooling fishes over a wide range of water velocities (0.3–8.0 body lengths $s^{-1}$; BL $s^{-1}$), and then compared the swimming performance curve to that of solitary fish. We equipped a high-resolution (*see* Methods for our approach to enhancing the signal-to-noise ratio in our respirometer) swim-tunnel respirometer with two orthogonal high-speed cameras to quantify three-dimensional (3-D) fish kinematics. This enabled us to simultaneously measure energetics, 3-D dynamics of fish schools (n=5 replicate schools), and the kinematics of solitary fish (n=5) of a model species, giant danio (*Devario aequipinnatus*), that exhibits an active directional group swimming from near still water to maximum sustained speeds (equivalent to a Reynolds number range of $6.4 \cdot 10^3$ to $1.8 \cdot 10^5$; Fig. S2), using a $U_{crit}$ test.

**Results**

We discovered that both solitary fish and fish schools have a concave upward shaped aerobic metabolic rate ($\dot{M}O_2$)-speed curve over the lower portion of their speed range (0.3–3 BL $s^{-1}$, Fig. 2C, D). The aerobic locomotor cost at 0.3–3 BL $s^{-1}$ showed no statistical difference between solitary fish and fish schools ($F_{1,80} \leq 2.40$, $p \geq 0.13$). Fish schools swimming at ~1.0 BL $s^{-1}$ consume less energy than at slower speeds ($F_{9,40} = 24.7$, $p \leq 0.0007$), while swimming at 3 BL $s^{-1}$ consumes a similar amount of energy to maintain position at a water velocity of 0.3 BL $s^{-1}$ ($p = 0.85$; Fig. 2D). Danio schools have a minimum aerobic cost ($\dot{M}O_{2min}$ = 212.9 mg $O_2$ $kg^{-1}$ $h^{-1}$) of 1.25 BL $s^{-1}$. $\dot{M}O_{2min}$ at this optimal speed ($U_{opt}$) was *lower* than both the $\dot{M}O_2$ of aggregating behaviours (328.5 mg $O_2$ $kg^{-1}$ $h^{-1}$) exhibited before $U_{crit}$ test (Table S1, Fig. S3) and for the group at rest in still water $\dot{M}O_2$ (267.9 mg $O_2$ $kg^{-1}$ $h^{-1}$) (by 35% and 21% respectively; $F_{2,12} = 16.7$, $p \leq 0.02$, Fig. 2A, B). Swimming at $U_{opt}$ reduces the energetic cost below that of swimming at either

142 slower or higher speeds. Indeed, the Strouhal number of fish schools decreased from 2.1 at the
143 lowest speed to 0.3 at the energetic minimum $U_{opt}$, and then increased to 0.4 at the higher $U_{crit}$.
144 We also characterized the kinematic features that result in elevated $\dot{M}O_2$ at low water
145 velocities. Danio maintaining body position in low-velocity aggregations had a higher tail beat
146 frequency ($f_{TB}$) than solitary fish ($F_{1,80} \geq 9.8$, $p \leq 0.002$). However, at $U_{opt}$ and the highest speed
147 of active directional schooling, fish in schools had a lower $f_{TB}$ ($F_{1,80} \geq 4.6$, $p \leq 0.035$) than
148 solitary fish (Fig. 4B). The 3-D angular heading of schooling fish transitioned from
149 omnidirectional to pointing against water flow when water velocity is above 0.75 BL $s^{-1}$, and
150 individual fish orient into the flow starting at 0.3 BL $s^{-1}$ (Fig. 4C). Although the body angle and
151 turning frequency of solitary fish and schools decreased with water velocity, schooling fish had a
152 higher turning frequency ($F_{1,80} \geq 15.6$, $p < 0.002$) below 0.75 BL $s^{-1}$ than solitary fish (Fig.
153 4D,E).
154 We discovered that, across the entire 0.3–8 BL $s^{-1}$ range, $\dot{M}O_2$-speed curves of fish
155 schools are concave upward shaped (reached 1053.5 mg $O_2$ $kg^{-1}$ $h^{-1}$ at 8 BL $s^{-1}$) whereas solitary
156 fish showed an upward concave curve that reaching a plateau of 760.2 mg $O_2$ $kg^{-1}$ $h^{-1}$ (~10% CV
157 in 6–8 BL $s^{-1}$, Fig. 2C), demonstrating that schooling dynamics results in a 44% higher
158 maximum aerobic performance ($F_{1,80} = 30.0$, $p < 0.001$). This increased maximum aerobic
159 performance translated to a lower use of aerobic capacity compared to solitary fish over 0.3–8
160 BL $s^{-1}$ (*see* the discussion for how fish swimming in school can improve aerobic performance).
161 Collectively, fish schools used a 36% lower proportion of their aerobic scope than solitary fish
162 (Wilcoxon test: $p = 0.0002$, Fig. 2F). Fish schools used a 38% lower proportion of aerobic scope
163 (34 vs. 55%) at 4 BL $s^{-1}$ (50% $U_{crit}$ & > 50% aerobic scope onward), and consistently used ~25%
164 lower proportion of their aerobic scope at 6 and 7 BL $s^{-1}$ than solitary fish ($F_{1,103} \geq 4.8$, $p \leq 0.03$,
165 Fig. 2E).

166 Given that fish schools had a higher maximum aerobic performance, generally used a
167 lower proportion of their aerobic scope, and individuals within the schools have a 14% lower $f_{TB}$
168 than the solitary fish at 8 BL $s^{-1}$ (11.5 vs. 13.3 Hz, $F_{1,80} = 15.1$, $p < 0.001$), we predicted that fish
169 schools, compared with solitary fish, use less anaerobic energy to supplement aerobic energy for
170 the high-speed movement approaching their aerobic limit. Hence, we measured post-exercise $O_2$
171 utilization, a majority of which is used to restore high-energy phosphate storage and
172 glycolytically induced metabolic perturbations (EPOC: Excess Post-exercise $O_2$ Consumption).
173 We discovered that fish schools have a 65% lower EPOC (0.69 vs. 1.95 mg $O_2$; $t_8 = 4.5$, $p =$
174 0.0021), and recover 43% faster than solitary fish (8 vs. 14 h; $t_8 = 2.8$, $p = 0.025$; Fig. 2G, H).
175 To estimate the relative proportions of aerobic and anaerobic energy contributions for
176 locomotion at each swimming speed, we modeled EPOC in addition to $\dot{M}O_2$, the aerobic cost (>
177 50% $U_{crit}$ & aerobic scope, Fig. 3A) (Table S2). We also estimated the total $O_2$ cost during the
178 entire swimming process for each school and individual and calculated total energy expenditure
179 (TEE) (*10*). The TEE of fish schools was 38–53% lower than that of the solitary fish between 5–
180 8 BL $s^{-1}$ ($F_{1,103} \geq 7.4$, $p \leq 0.008$; Fig. 3D). TEE of fish schools was only 42–143 % higher than
181 the aerobic metabolic rate at 5–8 BL $s^{-1}$ ($F_{1,96} \geq 3.5$, $p \leq 0.001$) and anaerobic metabolic energy
182 only accounted for 29–58 % of the TEE depending on speed (Fig. 3B). In contrast, TEE of
183 solitary fish was 131–465 % higher than the aerobic metabolic rate between 5–8 BL $s^{-1}$ ($F_{1,112} \geq$
184 10.7, $p \leq 0.001$), where anaerobic energy accounted for 62–81% of the TEE depending on speed
185 (Fig. 3C).
186 Schooling dynamics reduced the total cost (aerobic plus anaerobic) of transport (TCOT)
187 by an average of 43% compared to swimming alone ($F_{1,103} = 6.9$, $p = 0.01$), and most of this
188 energy conservation happens at higher speeds when fish approach their aerobic limit. Schooling
189 dynamics in danio enables an extremely shallow rate of increase in TCOT with speed compared

to that of an individual (Fig. 3E). The TCOT of solitary fish increased by 490% (6.5 kJ $km^{-1}$ $kg^{-1}$) at 8 BL $s^{-1}$, whereas the schooling TCOT increased by only 200% (3.6 kJ $km^{-1}$ $kg^{-1}$) at 8 BL $s^{-1}$. Therefore, individual fish form a more energy-efficient biological entity when they collectively move as a school.

To answer the question of how schooling dynamics reduces TEE, we combine video analysis of fish tail beat kinematics with simultaneous aerobic and anaerobic measurements to compute energy expended *per tail beat* (TEE•$beat^{-1}$), and compared values for fish in schools to those for solitary fish. Schooling fish reduced TEE•$beat^{-1}$ by 30–56% at higher speeds compared to solitary fish ($F_{1,81} \geq 7.3$, $p \leq 0.008$), a substantial reduction in TEE•$beat^{-1}$ consumed both by the school, and by individual fish within a school (Fig. 4A). Notably, the energetic benefits during active directional schooling occur when fish schools become more streamlined, as the length of fish school increased with speed and plateaued beyond 2 BL $s^{-1}$ (Fig. 4F), while the 3-D distance among individuals stayed relatively constant at ~1.2 BL (Fig 4G). These results directly demonstrate schooling dynamics benefits the swimming kinematics of individual fish within the school and results in a net outcome of up to 53% TEE reduction in fish schools compared to solitary fish.

## Discussion

Simultaneous characterization of energetics and kinematics enables an integrated understanding of both the physiology and physics of fish schooling behaviour. Hydrodynamic models, kinematic measurements, and robotic analyses of fish schools indicate that the cost of swimming can be reduced when fish swim beside neighbouring fish (*20*), behind or in front of another fish (*24*), or behind leading individuals (*6*) (Fig. 1). We have demonstrated here that fish schools downshifted an overall concave upward swimming energetics performance curve at

214 higher speeds by ~43%. Energy use as swimming speed increases changes in a non-linear
215 manner, with higher energy use at the lowest speeds (Fig. 2D), and the performance curve below
216 3.0 BL $s^{-1}$ is *U*-shaped. Energy saving occurs through a substantial reduction in the non-aerobic
217 energy contribution when fish approach aerobic limits. One of the key ecological benefits of the
218 reduced use of glycolysis is a faster recovery time from fatigue (Fig. 2H). This would enable fish
219 schools in nature to repeat high-performance movements. Considering that high-speed
220 maneuvers are extremely common in predatory evasion (*25*) food-searching group motion (*26*),
221 and in fish schools in the ocean (Fig. S1), energy savings by fish schooling at high speed and the
222 faster recovery that followed could have a considerable impact on lifetime fitness (*27*) (*28*).
223 Moreover, considerable energy savings occur even though we observed that individual danio
224 regularly change positions within the school and do not maintain stable inter-individual
225 locations. We expect that this is because individuals within the school can use multiple
226 hydrodynamic mechanisms to save energy depending on their location (Fig. 1). We propose that
227 energetic savings by collective movement may not require either fixed positional arrangements
228 among individuals or specific kinematic features (such as tail beat synchronization) compared to
229 solitary locomotion. Based on these results, we regard fish schooling as a highly robust
230 behaviour that provides considerable energetic benefits that are not necessarily sensitive to
231 specific fish locations or movements. Future studies are necessary to decipher each of the
232 specific hydrodynamic mechanisms for energy saving.
233
234 **Schooling dynamics enhances aerobic performance and reduces non-aerobic energy use**
235 We discovered that a significant amount of energy conservation for active directional
236 swimming occurs at speeds above 3 BL $s^{-1}$. In nature, fish schools routinely exhibit active
237 directional collective locomotion above ~6 BL $s^{-1}$ (Fig. S1, Table S3) (*29*), a speed that engages

anaerobic glycolysis. Yet, there are no previous measurements of the anaerobic cost of schooling in fish. Hence, important and previously unrecognized benefits of active directional collective locomotion are (1) increased aerobic performance, (2) a reduced use of aerobic capacity and anaerobic energy, and (3) a resultant faster recovery from the associated metabolic perturbations and costs of swimming at higher speeds. When animals are approaching their maximum metabolic rate, the highest attainable rate of $O_2$ uptake limits aerobic performance during the unsteady state of high-speed locomotion and anaerobic glycolysis is engaged to support the maximum metabolic demand.

Fish swimming at higher speeds (> 50% $U_{crit}$) routinely exhibit a burst-&-glide gait mode of locomotion (*30*, *31*). Repeated bursting is substantially fueled by anaerobic glycolysis and the gliding phase enables peak $\dot{M}O_2$ (*32*) to replenish the venous $O_2$ content (*33*). Fish within a school are known to increase gliding time and decrease burst time by 19% when they are trailing the leading fish (*34*), *e.g,* a lower $f_{TB}$ of fish schools at 8 BL $s^{-1}$ is related to the extended gliding time (Fig. 4B). We reason that the higher proportion of time spent gliding likely enables more bouts of peak $\dot{M}O_2$ and enhances the maximum aerobic performance (*32*) (*33*). This enhanced maximum aerobic performance increases the metabolic ceiling and enables fish to use a lower proportion of their aerobic scope for locomotion (Fig. 2E). Physiological studies of exercise metabolism and locomotion suggest that a lower proportional use of aerobic scope during movement relates to a reduced accumulation of anaerobic end-products (*9*). Collectively, our results showed that the increased aerobic performance (Fig. 2C) and the reduced use of the aerobic capacity (Fig. 2E) for swimming above 50% $U_{crit}$ in fish schools likely plays a key role in reducing the use of glycolysis and the accumulation of lactate (*e.g.* EPOC, Fig. 2G) for high-speed swimming (*10*, *31*).

261 We present direct evidence of substantial non-aerobic energy saving by demonstrating
262 the 65% lower EPOC (Fig. 2G) used by fish that swam in schools. Anaerobic glycolysis is
263 crucial in permitting continued movement when aerobic limits are reached at high swimming
264 speeds (*35*). Often vertebrates at higher speeds use more fast twitch fibres that generate high-
265 frequency contractile force in part through anaerobic glycolysis (*36*) (*37*). The higher EPOC for
266 single fish is unlikely to have been confounded by any possible stress effect of swimming as a
267 solitary fish. Stressed solitary fish would have elevated aerobic metabolic rates in low water
268 velocity, which we show is not the case for our experiments (*see* Fig. 2D). Indeed, to mitigate the
269 stress response, we acclimated fish to the solitary conditions and habituated fish to the
270 respirometer for a quiescent day before the experiment (*see* more details in experimental animal
271 and protocols). When vertebrates move at high speed, the typical 'stress' neurotransmitters (*e.g.*
272 adrenaline, catecholamines & cortisol) usually increase (*38*) (*39*), regardless of whether
273 vertebrates move as an individual or in a group. These endocrinological responses underpin the
274 physiological mechanisms that enable higher aerobic performance (*e.g.* rising heart rate) (*40*)
275 (*41*). Moreover, after the highest swimming speeds immediately followed by an active recovery
276 process, fish likely prioritize the recovery of the essential functions (as the levels of the
277 neurotransmitters decline fairly rapidly) for the potential of repeated locomotion performance
278 (speedy recovery allows fish to restore their swimming performance) (*31*) (*42*) (*43*).
279 To present a complete energetic profile showing the total energy expenditure (TEE) of
280 locomotion for fish schooling, we model the non-aerobic cost (EPOC) on top of the aerobic
281 swimming performance curve. The model is rooted in the use of aerobic and glycolytic energy
282 when fish swim above 50% $U_{crit}$ (*30*) and a commonly observed inflection point of faster
283 anaerobic end-product accumulation is at ~50% aerobic scope (*9*) (*see* Methods for detailed
284 physiological bases and criteria for EPOC modeling). As a result, we observed a TEE being ~2.5

285 fold higher than the aerobic metabolic energy expenditure which agrees with the theoretical
286 estimates based on individual yearling sockeye salmon (*44*). This model elucidates how aerobic
287 and anaerobic metabolic energy constitute TEE, fuel muscles, generate locomotor thrust and
288 overcome hydrodynamic drag during swimming.

289 We also demonstrated that the need for energy saving in fish schools at lower speeds (< 3
290 BL $s^{-1}$ or 38% $U_{crit}$ Fig. 2E, 3D, E) is not as crucial as at higher speeds where we demonstrated
291 substantial energy savings in the schools compared to solitary individuals. Fluid drag is
292 exponentially less at lower speeds compared to higher speeds. Fish predominately use aerobic
293 metabolism to support low-speed steady swimming for prolonged periods (*10*) which does not
294 require lengthy recovery as swimming at higher speeds where glycolysis contributes to the
295 energetic demands. The costs of low-speed swimming are often less than < 20% of aerobic
296 capacity (Fig. 2E), which leaves the majority of aerobic capacity (>50%) for other activities.
297 Therefore, the benefits of reducing the energetic cost of locomotion are likely not major factors
298 underlying behaviours such as low-speed milling (*45*) and aggregation (*46*) in fishes, where other
299 ecological drivers such as feeding, predator avoidance, and reproduction likely dominate the
300 fitness landscape.

301

302 **Schooling dynamics and energy conservation**

303 Our 3D kinematic analyses shed light on the complex interactions between schooling and
304 hydrodynamics that enable energy saving by fish collective movement. One of the key possible
305 mechanisms is local interactions among individuals, where the kinematics of individual fish
306 respond to the wakes shed by neighbours (*47*). Kinematic and simulation studies indicate that 2–
307 3 coordinated fish can save energy (*48*) (*20*) through local interactions. We directly demonstrate
308 here that eight coordinated fish can save energy, and recent simulations show that schooling

309 benefits can extend to at least 23 fish (*21*). Although these studies appear to suggest that the
310 energetic benefits of schooling are scalable, we are still some ways from proving the exact
311 mechanisms of how the large school size in nature is coordinated and whether or not local
312 interactions are still one of the mechanisms for energy saving when scaling up school size.
313 Future hydrodynamic and long-term 3-D tracking studies are needed to investigate the specific
314 schooling formations and hydrodynamic mechanisms used by live fish for energy saving (as
315 summarized in Fig.1) (*49*).

316 We show that danio in a school keep a relatively consistent 3-D distance from neighbours
317 and have small variation in mean position even as individuals routinely change position within
318 the school (Fig. 4G). Computational fluid dynamic analyses of fish schools show that a small 3D
319 neighbouring distance (*e.g.* < 0.4 BL $s^{-1}$) increases drag and can increase swimming costs,
320 whereas a large 3-D neighbouring distance (*e.g.* > 2 BL $s^{-1}$) reduces the hydrodynamic benefits
321 (*48*). There may thus be an optimal mean distance among individuals within a school to
322 maximize energetic savings. Whether inter-individual distance should change as swimming
323 speed increases remains an open question and may be a function of school size. While we cannot
324 completely preclude the possibility that elongation of danio fish school might be due to the
325 weaker individuals falling behind, the fact that the school maintained a stable 3-D distance as
326 speed increased and that fish continued to change position within the school suggests that the
327 elongated school volume at higher speeds may reflect changing hydrodynamic interactions
328 among individuals (Fig. 1).

329 To encapsulate the complex interaction among animal physiology, kinematics and fluid
330 dynamics, more comprehensive quantification beyond simple kinematic metrics are necessary.
331 For example, the wing flapping frequency of birds in a V-formation can be higher than for
332 solitary flight despite strong indirect evidence of overall energy saving by V-formation flying (*2*)

333 (*12*) (*19*), and flapping phase of adjacent birds may be informative for understanding the fluid
334 dynamic advantages of V-formation flying (*12*). Likewise, phase matching of body motion
335 between neighbouring fish can help individual fish within the school to boost thrust or reduce
336 drag (*20*). Fish can also adjust their body stiffness and maintain $f_{TB}$ while reducing the amount of
337 muscle activity needed to generate movement (*50*) (*51*) (*52*). Thus, we did not observe consistent
338 and substantial changes in the $f_{TB}$ of fish within the schools compared to solitary swimmers
339 despite demonstrating substantial energetic savings by the group at high speed. Although
340 reduced $f_{TB}$ has been used in past studies as an indirect indicator of energy saving in fishes (*53*)
341 (*54*), we caution that $f_{TB}$ is not necessarily an indicator of energy use in group dynamics where
342 fish constantly and dynamically interact with complex vortices and flow generated by other
343 individuals. By simultaneously measuring kinematics and energetics, we discovered a
344 downshifted performance curve of TEE per tail beat in fish schools at higher speeds (Fig. 4A),
345 even with limited alteration in $f_{TB}$ at lower swimming speeds within the school. This suggests
346 that the locomotor muscle fibres in the body musculature of fish within the school need to
347 generate less force as indicated by the lower measured TEE. Fish can possibly fine-tune
348 undulatory motion to harness kinetic energy from nearby vortices (*20*) (*48*), reducing biological
349 energy contribution for thrust.
350

351 **Aerobic metabolic rate–speed curve of fish schools**

352 We discovered that the aerobic metabolic rate ($\dot{M}O_2$)–speed curve at speeds less than 3
353 BL $s^{-1}$ is *U*-shaped, with swimming at 0.3 BL $s^{-1}$ utilizing the same aerobic energy as moving at 3
354 BL $s^{-1}$ (Fig. 2D). The entire aerobic energy-speed performance curve is concave upward in an
355 extended *J*-shape (Fig. 2C), and non-linear, in contrast to several previous analyses of energy use
356 with speed in fish which have shown linear relationships (*55*) (*56*) (*57*). By quantifying energy

use over a wide speed range and by measuring aerobic energy use at 14 distinct speeds, we showed that locomotion at the lowest speeds involves increased energy use relative to swimming at speeds up to 3 BL $s^{-1}$, similar to previous results from skate locomotion (*58*). This suggests that analyses of fish energy use as speed increases would benefit from increasing the number of tested speeds, and that efforts to extend speed measurements to both the lowest and highest speeds would enable a greater level of precision in measuring fish locomotor performance.

One key finding in this regard is that fish schools show a minimal absolute energetic cost ($\dot{M}O_2$) at a mean group swimming speed of ~1.0 BL $s^{-1}$ that is higher than the minimum swimming speeds tested. Thus, fish schools can swim at a speed with the least amount of energy use and potentially extend the distance travelled with the same amount of metabolic substrate onboard. This swimming speed of minimum cost closely matches the migratory speeds of carangiform and subcarangiform migratory fishes (often as schools) which are in the range of 0.5 to 1.5 BL $s^{-1}$ as recorded by tags on migrating fish (*59*, *60*) (Fig. S1; Tables S1, S3). Although *D. aequipinnatus* is not a migratory species, our results suggest that the migratory speed of fish schools likely occurs at the speed showing the minimum aerobic metabolic rate for long-distance locomotion. Indeed, the Strouhal number when fish schools swim at $U_{opt}$, showing a minimum aerobic energy cost of locomotion, is 0.3, a hallmark of efficient swimming for many fish species (*61*). Fish of different size swimming at 1 BL $s^{-1}$ will necessarily move at different Reynolds numbers, and hence the scaling of body size to swimming speed needs to be considered in future analyses of other species that differ in size.

The exact energetic mechanisms underpinning the chosen migratory speeds of fish schools would benefit from more in-depth studies. Since both fish schools and solitary individuals have $U_{opt}$ of ~1 BL $s^{-1}$, the $\dot{M}O_2$–speed curve of a fish school might be the average of individual curves from fish within the school. However, pushing and pulling forces from

381 hydrodynamic interactions of neighbouring fish could help swimmers settle into stable
382 arrangements, a phenomenon known as the Lighthill conjecture (*62*). Further studies will need to
383 explore whether individuals within the school are more frequently located at points
384 recommended by the Lighthill conjecture which could potentially result in minimum metabolic
385 costs of locomotion at $U_{opt}$ in fish schools (*49*). Research on fish swimming in large aquaculture
386 circular tanks has discovered that holding a large school of salmonids at a water velocity of ~1
387 BL $s^{-1}$ resulted in healthy growth and good conditions (*63*). This phenomenon seems to suggest
388 that the minimum metabolic costs of locomotion yield the largest available aerobic capacity for
389 growth and other functions.

390 Higher locomotor costs at the lowest speeds are likely caused by higher postural costs for
391 active stability adjustments in the near-still fluid. The direct link between higher energetic costs
392 caused by a higher 3-D body angle and higher turning frequency at the lowest speeds in solitary
393 danio (Fig. 4D, E) supports previous results in skates (*58*) where energetic costs are high at the
394 very low swimming speeds due to the increased energetic cost involved in maintaining body
395 stability and generating lift in negatively buoyant fishes. We expect more species that move in
396 the fluid to show a higher postural cost in near-still fluid but careful measurements of both body
397 kinematics and position along with high-resolution respirometry and accurate low-speed flow
398 control will be required to demonstrate this phenomenon in a diversity of fish species. Elevated
399 costs should be indicated at the lowest speeds as a direct increase in $\dot{M}O_2$ and not just as COT.
400 When the denominator (*i.e.* speed) for deriving COT is less than 1, COT tends to skew towards
401 the higher value at the lowest speeds. Mechanistically, fish at low fluid speeds have lower
402 muscle and propeller efficiencies (*44*) with reduced fluid-assisted stability. Increased active
403 stability adjustments such as fin movements (*58*) and tilting behaviours that enable the fish's
404 body to act as a hydrofoil (*64*) are used for stability control (see supplementary video).

405 Moreover, danio do not show intermittent swimming gaits at low speed as observed in some
406 labriform swimmers (*65*) (*66*), and hence gait-specific kinematics most likely do not play a role
407 in the elevated locomotion cost that we observe at the lowest speeds. Also, the higher turning
408 frequency at < 0.75 BL $s^{-1}$ in fish schools can relate to the need for coordination with neighbours.
409 Nevertheless, as fish move more rapidly over a speed range, we note that the total cost of
410 transport of ~1.2 kJ $km^{-1}$ $kg^{-1}$ at 3 BL $s^{-1}$ is among the lowest recorded for aquatic organisms, and
411 is less than the TCOT (1.5 kJ $km^{-1}$ $kg^{-1}$) for jellyfish (the most energetically efficient low-speed
412 swimmers) (*4*) swimming at < 2 BL $s^{-1}$ (*67*).
413
414 In summary, our experiments on giant danio have demonstrated substantial energy
415 conservation resulting from schooling dynamics across a wide range of speeds in fish. Direct
416 measurement of both aerobic and non-aerobic energy use is critical for understanding the rapid
417 collective movement of animals. Fish schooling in the high-drag viscous aquatic medium serves
418 as a model for understanding how group movement by animals can be a more energy-efficient
419 biological collective than movement by isolated individuals. By increasing maximum aerobic
420 performance, fish schools save anaerobic energy and reduce the recovery time after peak
421 swimming performance. Furthermore, by decreasing the proportion of metabolic capacity and
422 recovery time devoted to locomotion, animals can apportion more energy to other fitness-related
423 activities, such as digestion, growth and reproduction. More broadly, comprehending how the
424 collective dynamics of animal movements in the water, land, and air can modify the energy use
425 profiles of individuals provide a better understanding of the ecological and evolutionary
426 implications of group locomotion.
427

428 **Materials and Methods**

429 **Experimental animals**

430 The experiments were performed on giant danio (*Devario aequipinnatus*) that were
431 acquired from a local commercial supplier near Boston, Massachusetts USA (Table S4). Five
432 schooling groups are randomly distributed and housed separately in five 37.9 l aquaria (n=8 per
433 tank). The five solitary individuals are housed separately in five 9.5 l aquaria (n=1 per tank). The
434 individual housing condition acclimated the single *D. aequipinnatus* to the solitary environment
435 and helped to reduce any isolation stress that might elevate whole-organism metabolic rate. In
436 fact, the aerobic locomotion cost of solitary individuals showed no statistical difference from (in
437 fact, being numerically lower) that of fish schools at a very low testing speed. The flow speed is
438 similar to some areas of the aerated home aquarium for each individual fish. This suggests that
439 the stress of solitary fish likely does not meaningfully contribute to the higher locomotor costs
440 (*see* experimental protocol for more details on mitigating the stress). The condition factor
441 showed no difference between solitary fish and fish schools (0.81 vs. 0.99; $t_8 = 2.14$, $p = 0.065$).
442 All aquaria have self-contained thermal control (28 °C), an aeration system (>95 % air
443 saturation, % sat.) and a filtration system. Water changes (up to 50% exchange ratio) were
444 carried out weekly. Fish were fed *ad libitum* daily (TetraMin, Germany). Animal holding and
445 experimental procedures were approved by the Harvard Animal Care IACUC Committee
446 (protocol number 20-03-3).

447

448 **Integrated Biomechanics & Bioenergetic Assessment System (IBAS)**

449 The core of our Integrated Biomechanics & Bioenergetic Assessment System (IBAS) (Fig.
450 S4) is a 9.35-l (respirometry volume plus tubing) customized Loligo® swim-tunnel respirometer
451 (Tjele, Denmark). The respirometer has an electric motor, and a sealed shaft attached to a

452 propeller located inside the respirometer. Regulating the revolutions per minute (RPM) of the
453 motor controls water velocity of the tunnel. The linear regression equation between RPM and
454 water velocity (V) is established ($V = 0.06169 \bullet RPM - 5.128$, $R^2 = 0.9988$, $p < 0.0001$) by
455 velocity field measured by particle image velocimetry (PIV). Hence, the aerobic costs during
456 locomotion are measured through the regulation of the water velocity.

457 The swim-tunnel respirometer is oval-shaped. The central hollow space of the respirometer
458 increases the turning radius of the water current. As a result, the water velocity passing the cross-
459 section of the swimming section (80 × 80 × 225 mm) is more homogenous (validated by direct
460 particle image velocimetry (PIV) of flow in the working section of the respirometer following
461 the procedures in (*68*)). Moreover, a honeycomb flow straightener (80 × 80 × 145 mm) is
462 installed in the upstream section of the swimming section that was specifically designed to create
463 relatively uniform flow across the working section (also confirmed by direct flow imaging).
464 Based on our flow visualization analyses, the effective distance of slow-moving fluid due to
465 boundary layer was <2.5mm at speeds above 2 BL $s^{-1}$. The boundary layer played an ever-
466 diminishing role at higher speeds (> 4 BL $s^{-1}$) when energy saving of fish schools becomes more
467 predominant. Danio (~10 mm wide) cannot effectively hide in the narrow boundary layer created
468 by our flow baffle system. In addition, the convex hull volume of the fish school did not change
469 as speed increased, suggesting that the fish school was not flattening against the wall of the swim
470 tunnel, a typical feature when fish schools are benefiting from wall effects. In nature, fish in the
471 centre of the school effectively swim against a 'wall' of surrounding fish where they can benefit
472 from hydrodynamic interactions with neighbours.

473 To standardize the experimental apparatus and avoid instrument variation, solitary fish and
474 fish schools are measured in the same swim-tunnel respirometer, and the same overall
475 experimental design is used as in previous studies (*14*) (*13*) (*15*). The ratios of

476 respirometer:individual volume ($r_{RI}$) in our experiments was 2200 for individual fish (we used
477 larger solitary *D. aequipinnatus* to increase the signal-to-noise ratio), and 693 for fish schools.
478 The $r_{RI}$ is essentially a balance between giving enough space for fish to exhibit natural
479 locomotion and reducing wall effects and generating a reliable signal-to-noise ratio to measure
480 the decline of dissolved $O_2$ (DO) in water (*69*). The increase in the signal-to-noise ratio can come
481 from the better technology of the $O_2$ probe (we used an optical $O_2$ probe which has a higher
482 measurement sensitivity than the Winkler method or Electrode & Galvanic probes used in the
483 previous studies, *see* (*70*) for review) and modifications to the swim-tunnel respirometer. We
484 used a water loop is installed 95 cm downstream of the propeller with water returned to the
485 respirometer 240 cm upstream of the swimming section. Flow in the water loop moves
486 (produced by an in-line circulation pump, Universal 600, EHEIM GmbH & Co KG, Deizisau,
487 Germany) in the same direction as the water flow in the swimming tunnel. A high-resolution
488 fibre optic $O_2$ probe (Robust oxygen probe OXROB2, PyroScience GmbH, Aachen, Germany) is
489 sealed in the loop in the downstream of the circulation pump where there is better mixing to
490 continuously measure the DO level in the water (recording frequency ~1 Hz, response time <
491 15s). The designated water sampling loop together with the water mixing by the propeller and
492 water pumps effectively reduces the noise-to-signal ratio. As a result, the respirometry system
493 reaches a stable signal-to-noise ratio once the sampling window is longer than 1.67 mins (*see*
494 Fig. S5), well within the duration of the velocity step to obtain a stable signal-to-noise ratio for
495 calculating $\dot{M}O_2$ (*32*).

496 The oxygen probe was calibrated to anoxic (0 % sat., a solution created by super-saturated
497 sodium sulphite and bubbling nitrogen gas) and fully aerated water (100 % sat.). After fish
498 removal, the background $\dot{M}O_2$ in the swim-tunnel respirometer was measured for a 20-min
499 sealed period before and after each trial to calculate the average background $\dot{M}O_2$ (< 6% of fish

500 $\dot{M}O_2$), which was used to correct for the $\dot{M}O_2$ of fish (*69*). The pre-filtered water (laboratory
501 grade filtration system) is constantly disinfected by UV light (JUP-01, SunSun, China) located in
502 an external water reservoir to suppress the growth of microbial elements. Water changes of 60%
503 total volume occurred every other day and a complete disinfection by sodium hypochlorite is
504 conducted weekly (Performance bleach, Clorox & 1000 ppm).

505 To simultaneously measure schooling dynamics and swimming kinematics, the customized
506 oval-shaped swim-tunnel respirometer is located on a platform with an open window beneath the
507 swimming section. The platform is elevated 243 mm above the base to allow a front surface
508 mirror to be installed at a 45° angle. This mirror allows a high-speed camera (FASTCAM Mini
509 AX50 type 170K-M-16GB, Photron Inc., United States, lens: Nikon 50mm F1.2, Japan) to
510 record the ventral view. The second camera (FASTCAM Mini AX50 type 170K-M-16GB,
511 Photron Inc., United States, lens: Nikon 50mm F1.2, Japan) is positioned 515 mm to the side of
512 the swimming section to record a lateral view. Synchronized lateral and ventral video recordings
513 were made at 125 fps, and each frame was 1024 by 1024 pixels. To avoid light refraction passing
514 through the water and distorting the video recordings, the swim-tunnel respirometry is not
515 submerged in a water bath. Temperature regulation of the respirometer is achieved by regulating
516 room temperature, installing thermal insulation layers on the respirometer and replenishing the
517 water inside the respirometer from a thermally regulated (28 °C, heater: ETH 300, Hydor, United
518 States & chiller: AL-160, Baoshishan, China) water reservoir (insulated 37.9-l aquarium) located
519 externally.

520 The aerated (100% sat., air pump: whisper AP 300, Tetra, China) reservoir water is flushed
521 (pump: Universal 2400, EHEIM GmbH & Co KG, Deizisau, Germany) to the respirometer
522 through an in-line computer-controlled motorized ball valve (U.S. Solid) installed at the in-flow
523 tube. The other in-line one-way valve is installed at the out-flow tube. The out-flow tube is also

524 equipped with a one-way valve. The valve is shut during the measurement period, a
525 precautionary practice to eliminate the exchange of water between the respirometer and the
526 external reservoir when the water moves at a high velocity inside the respirometer. This flushing
527 was manually controlled to maintain DO above 80 % sat. Every time the respirometer was closed
528 to measure $\dot{M}O_2$, the water temperature fluctuates no more than 0.2 °C. The water temperature
529 inside the respirometer is measured by a needle temperature probe (Shielded dipping probe,
530 PyroScience GmbH, Aachen, Germany) sealed through a tight rubber port of the respirometer.
531 To allow fish to reach the undisturbed quiescent state during the trial (another stress
532 mitigation practice), the entire IBAS is covered by laser blackout sheets (Nylon Fabric with
533 Polyurethane Coating; Thorlabs Inc, New Jersey, United States). The room lights are shut off
534 and foot traffic around IBAS is restrained to the absolute minimum. Fish are orientated by dual
535 small anterior spots of white light (lowest light intensity, Model 1177, Cambridge Instruments
536 Inc, New York, United States) for orientation (one to the top and the other to the side) of the
537 swimming section. The test section is illuminated by infrared light arrays to allow high-speed
538 video recording with minimal disturbance of fish behaviour.
539

540 **Experimental Protocol**

541 The energy use of vertebrates at lower speeds is primarily aerobic, while for high-speed
542 movement anaerobic metabolic pathways are activated to supply the additional (largely shorter-
543 term) energy needs (*9*). While whole-animal aerobic metabolism is measured by oxygen ($O_2$)
544 uptake rate ($\dot{M}O_2$), the non-aerobic $O_2$ cost (mostly through high-energy phosphate and
545 anaerobic glycolysis) is measured as excess post-exercise $O_2$ consumption (EPOC)(*10*). Both
546 metabolic energy sources contribute to the total energy expenditure (TEE) required for
547 movement. For a given workload, the higher the maximum aerobic performance of the animal,

548 the less the need for the anaerobic energy contribution (*9*, *35*). The experimental protocol
549 captures both metabolic energy contributions by measuring $\dot{M}O_2$ during locomotion and EPOC
550 afterwards.

551 We studied five replicate schools and five replicate individuals. Swimming performance test
552 trials were conducted with *Devario aequipinnatus* fasted for 24 hours, a sufficient period for a
553 small size species at 28 °C (*i.e.* high resting $\dot{M}O_2$) to reach an absorptive state. In fact, we
554 observed no specific dynamic action, the amount of $O_2$ consumed for digestion during the first
555 diurnal cycle (Fig. S3). Prior to the swimming performance test, testing fish were gently weighed
556 and placed in the swim-tunnel respirometer. The fish swam at 35% $U_{crit}$ for 30 mins to help
557 oxidize the inevitable but minor lactate accumulation during the prior handling and help fish
558 become accustomed to the flow conditions in the swim-tunnel respirometer (*43*). After this time,
559 the fish to be tested were habituated (>20 hours) to the respirometer environment under quiescent
560 and undisturbed conditions. The long habituation period also helps to reduce the stress and
561 further reduce the likelihood that the solitary fish might be more stressed than the fish schools
562 and showed an elevated $\dot{M}O_2$ (*13*). During this time, we used an automatic system to measure the
563 resting $\dot{M}O_2$ for at least 19 hours. Relays (Cleware GmbH, Schleswig, Germany) and software
564 (AquaResp v.3, Denmark) were used to control the intermittent flushing of the respirometer with
565 fresh water throughout the trial to ensure $O_2$ saturation of the respirometer water. $\dot{M}O_2$ was
566 calculated from the continuously recorded DO level (at 1 Hz) inside the respirometer chamber.
567 The intermittent flow of water into the respirometer occurred over 930 s cycles with 30 s where
568 water was flushed into the respirometer and 900 s where the pumps were off and the
569 respirometer was a closed system. The first 240 s after each time the flushing pump was turned
570 off were not used to measure $\dot{M}O_2$ to allow $O_2$ levels inside the respirometer to stabilize. The

571 remaining 660 s when the pumps were off during the cycle were used to measure $\dot{M}O_2$. The in-
572 line circulation pump for water in the $O_2$ measurement loop stayed on throughout the trial.
573 We characterize the aerobic costs for the swimming performance of fish using an
574 established incremental step-wise critical swimming speed ($U_{crit}$) test (*10*). The first preliminary
575 trial determined the $U_{crit}$ of this population of *Devario aequipinnatus* as 8 BL $s^{-1}$. Characterizing
576 the swimming performance curve required a second preliminary trial to strategically select 9
577 water velocities (0.3, 0.5, 0.8, 1.0, 1.3, 1.5, 1.8, 2.3, 2.8 BL $s^{-1}$) to bracket the hypothesized
578 upward concave shaped aerobic metabolism-speed curve at the lower speed (< 40% $U_{crit}$).
579 Additional five water velocities (3.8, 4.9, 5.9, 6.9, 8.0 BL $s^{-1}$) are used to characterize the
580 exponentially increasing curve to the maximum and sustained swimming speed, $U_{crit}$ (*see* Fig.
581 S6). Altogether, 14 points provide a reliable resolution to characterize the swimming
582 performance curve. The cross-section of the danio school is ~10% of the cross-sectional area of
583 the swim tunnel, hence the blocking effect is negligible (*71*). At each water velocity, fish swam
584 for 10 mins (*58*) to reach a steady state in $\dot{M}O_2$ at low speed (*see* Fig. S7). Above 40% $U_{crit}$, $\dot{M}O_2$
585 can become more variable (*32*). Hence, in this protocol, we focus on measuring the sustained
586 aerobic energy expenditure by calculating the average $\dot{M}O_2$ for each 10-min velocity step using
587 Eqn 1. At the 5$^{th}$ min of each velocity step, both ventral and lateral-view cameras are triggered
588 simultaneously to record 10-sec footage at 125 frames per second, at 1/1000 shutter speed and
589 1024 ×1024 pixel resolution. Thus, both data streams of $\dot{M}O_2$ and high-speed videos are recorded
590 simultaneously. The $U_{crit}$ test is terminated when 12.5% of fish in the school or a solitary
591 individual touches the back grid of the swimming section for more than 20 secs (*43*). The $U_{crit}$
592 test lasted ~140 mins and estimates the aerobic portion of TEE over the entire range of
593 swimming performance.

To measure the contribution of non-aerobic $O_2$ cost, where the majority of the cost is related to substrate-level phosphorylation, and to calculate the TEE for swimming over the entire speed range, we measured EPOC after the $U_{crit}$ test for the ensuing 19 hours, recorded by an automatic system. Most previous measurements of EPOC have used a duration of ~5 hours (*see* review (*42*)), but our extended measurement period ensured that longer duration recovery $O_2$ consumption during EPOC was measured completely as fish were exercised to $U_{crit}$ (*see* summary table in *16*). The intermittent flow of water into the respirometer occurred over 30 s to replenish the DO level to ~95% sat. For the following 900 s the flushing pump remained closed, and the respirometer becomes a closed system, with the first 240 s to allow $O_2$ saturation inside the respirometer to stabilize. The remaining 660 s when the flushing pump was off during the cycle were used to measure $\dot{M}O_2$ (*see* Eqn. 1). The cycle is automated by computer software (AquaResp v.3) and provided 74 measurements of $\dot{M}O_2$ to compute EPOC. Upon the completion of the three-day protocol, the school or individual fish are returned to the home aquarium for recovery. The fish condition was closely monitored during the first 48 hours after the experiment, during which no mortality was observed.

**Bioenergetic measurement and modeling**

To estimate the steady-rate whole-animal aerobic metabolic rate, $\dot{M}O_2$ values were calculated from the sequential interval regression algorithm (Eqn. 1) using the DO points continuously sampled (~1 Hz) from the respirometer.

$$\dot{\mathrm{M}}\mathrm{O}_2 = \left[\frac{d_{DO_{[i,(i+a)]}}}{d_{t_{[i,(i+a)]}}} \bullet \left(V_r - V_f\right) \bullet S_O\right] / (t \bullet M_f) \qquad \text{(Eqn. 1)}$$

Where $^{d_{DO}}/_{d_t}$ is the change in $O_2$ saturation with time, $V_r$ is the respirometer volume, $V_f$ is the fish volume (1 g body mass = 1 ml water), $S_o$ is the water solubility of $O_2$ (calculated by AquaResp v.3 software) at the experimental temperature, salinity and atmospheric pressure, $t$ is a time constant of 3600 s $h^{-1}$, $M_f$ is fish mass, and $a$ is the sampling window duration, $i$ is the next $PO_2$ sample after the preceding sampling window.

To account for allometric scaling, the $\dot{M}O_2$ values of solitary fish were transformed to match the size of the individual fish in the school (*see* Table S4) using an allometric scaling exponent (b = 0.7546). The calculation of the scaling relationship [$Log_{10}(\dot{M}O_2) = b \bullet Log10(M) + Log10(a)$, where $M$ is the body mass & $a$ is a constant] was performed by least squares linear regression analysis ($y = 0.7546 \bullet x + 0.2046$; $R^2 = 0.6727$, $p < 0.0001$) on the 180 data points of metabolic rate and body mass from a closely related species (the best available dataset to our knowledge) . (The mass scaling for tail beat frequency was not conducted because of the lack of data for *D. aequipinnatus* and its related species. Using the scaling exponent of distant species for mass scaling of tail beat frequency will introduce errors of unknown magnitude.) The allometrically scaled $\dot{M}O_2$ values were used to derive other energetic metrics (listed below & such as aerobic scope) for the solitary fish. The energetic metrics of fish schools are calculated from the mass-specific $\dot{M}O_2$.

The resting oxygen uptake ($\dot{M}O_{2rest}$), the minimum resting metabolic demands of a group of fish or a solitary individual, is calculated from a quantile 20% algorithm (*74*) using the $\dot{M}O_2$ estimated between the $10^{th}$–$18^{th}$ hour and beyond the $32^{nd}$ –$51^{st}$ hour of the trial. These are the periods of quiescent state when fish completed the EPOC from handling and swimming test.

The $\dot{M}O_2$ for the aggregation (Fig. 2B, $\dot{M}O_{2aggregate}$) is calculated as the average value using the $\dot{M}O_2$ estimated between the $10^{th}$–$18^{th}$ hour without the effects of any tests.

639 Minimum oxygen uptake ($\dot{M}O_{2min}$) is the lowest $\dot{M}O_2$ value recorded in the entire trial,
640 which always occurred at the optimal speed when a school of fish collectively reached the lowest
641 $\dot{M}O_2$ value.
642 Active oxygen uptake ($\dot{M}O_{2active}$) is the highest average $\dot{M}O_2$ when fish are actively
643 swimming (*10*).
644 The aerobic scope (the metric for aerobic capacity) is the numerical difference between
645 $\dot{M}O_{2active}$ and $\dot{M}O_{2min}$ (*i.e.* $\dot{M}O_{2active} - \dot{M}O_{2min}$) (*10*).
646 The percentage of aerobic scope (% aerobic scope) is calculated by normalizing the $\dot{M}O_2$
647 value at a water velocity as a % aerobic scope: $[(\dot{M}O_2 - \dot{M}O_{2min}) / (\dot{M}O_{2active} - \dot{M}O_{2min})]*100\%$.
648 The apportioning of aerobic scope to swimming performance is computed across the entire range
649 of swim speeds.
650 The excess post-exercise oxygen consumption (EPOC) is an integral area of $\dot{M}O_2$ measured
651 during post-exercise recovery, from the end of $U_{crit}$ until reached $\dot{M}O_{2rest}$ plus 10% or within 24
652 hours post-exercise, whichever endpoint occurred first (*72*). This approach reduces the likelihood
653 of overestimating EPOC due to any potential spontaneous activities (*72*). To account for the
654 allometric scaling effect, we used the total amount of $O_2$ consumed (mg $O_2$) by the standardized
655 body mass of fish (1.66 g) for fish schools and solitary fish.
656 We model EPOC (*i.e.* non-aerobic $O_2$ cost) and $\dot{M}O_2$ during $U_{crit}$ to estimate a *total* $O_2$ cost
657 over the duration of the swimming performance test. Our conceptual approach was pioneered by
658 Brett (*10*) in fish (*75*) and is also used in sports science (*9*). Mathematical modeling of EPOC
659 and $\dot{M}O_2$ during swimming was applied to study the effects of temperature on the total cost of
660 swimming for migratory salmon (*43*). We improved the mathematical modeling by applying the
661 following physiological and physics criteria. The first criterion is that significant accumulation of
662 glycolytic end-product occurred when fish swimming above 50% $U_{crit}$ (*31*) which corresponds to

663 > 40% $\dot{M}O_{2max}$ (or ~ 50% aerobic scope) (*9*). This is also when fish start unsteady-state burst-&-
664 glide swimming gait (*31*). The second criterion is that the integral area for the non-aerobic $O_2$
665 cost during swimming can only differ by ≤ 0.09% when compared to EPOC. The non-aerobic $O_2$
666 cost during swimming is the area bounded by modeled $\dot{M}O_2$ and measured $\dot{M}O_2$ as a function of
667 time when fish swim > 50% $U_{crit}$ (*see* Fig. 2A & Table S2). The third criterion is that total energy
668 expenditure is expected to increase exponentially with swimming speed (Fig. S8). Specifically,
669 these curves were fitted by power series or polynomial models, the same models that describe the
670 relationship between water velocity and total power and energy cost of transport (Fig. S8).
671 Following these criteria, the non-aerobic $O_2$ cost at each swimming speed is computed by a
672 percentage (%) modifier based on the aerobic $O_2$ cost (Table S2). The exponential curve of total
673 $O_2$ cost as swimming speed of each fish school or solitary individual was derived by an iterative
674 process until the difference between non-aerobic $O_2$ cost and EPOC met the 2$^{nd}$ criterion. The
675 sum of non-aerobic $O_2$ cost and aerobic cost gives the total $O_2$ cost.

676 Total energy expenditure (TEE) is calculated by converting total $O_2$ cost to kJ × kg$^{-1}$ using
677 an oxy-calorific equivalent of 3.25 cal per 1 mg $O_2$ (*76*).

678 Cost of transport (COT), in kJ × km$^{-1}$ × kg$^{-1}$ is calculated by dividing TEE by speed (in km
679 × h$^{-1}$) (*58*).

680

681 **Three-dimensional kinematic data extraction from high-speed videography**

682 We used two synchronized 10-sec high-speed videos (lateral and ventral views, at each
683 speed) for kinematic analyses. We calibrated the field of view of the high-speed cameras using a
684 direct linear transformation for three-dimensional (3-D) kinematic reconstruction (DLTdv8)(*77*)
685 by applying a stereo calibration to the swimming section of the respirometer (*see* Fig. S9). We
686 digitized the anatomical landmarks of fish (*see* Fig. S10) to obtain the X, Y, and Z coordinates

for each marker at the 1st sec, 5th sec and 10th sec for videos recorded at each speed. These coordinates are used to calculate the following kinematic parameters. All the calculations are validated on the known length and angle of test objects inserted into the tank working section.

The 3-D distance between the tip of the nose of each fish in the school per frame is calculated in vector Eqn. 2

$$d = \sqrt{(Xa - Xb)^2 + (Ya - Yb)^2 + (Za - Zb)^2} \quad \text{(Eqn. 2)}$$

Where spatial coordinates of two neighbouring fish are ($X_a$, $Y_a$, $Z_a$) and ($X_b$, $Y_b$, $Z_b$) respectively.

The 3-D angle of each fish in the school to the frontal plane per frame is calculated by Eqn. 3

$$\theta = \arccos \frac{(X2-X1)\cdot(X3-X1)+(Y2-Y1)\cdot(Y3-Y1)+(Z2-Z1)\cdot(Z3-Z1)}{\sqrt{(X2-X1)^2\cdot(Y2-Y1)^2\cdot(Z2-Z1)^2}\cdot\sqrt{(X3-X1)^2\cdot(Y3-Y1)^2\cdot(Z3-Z1)^2}} \quad \text{(Eqn. 3)}$$

where the spatial coordinates of the caudal peduncle, nose of fish and right-angle crosshair between the peduncle and the nose are ($X_1$, $Y_1$, $Z_1$), ($X_3$, $Y_3$, $Z_3$) and ($X_2$, $Y_2$, $Z_2$) respectively (*see* Fig. S9).

The fish's angle to water flow per frame is calculated using the arctangent function in Excel (Microsoft, United States) using the spatial coordinates of the caudal peduncle and nose of the fish.

The school length (in *X*-axis) is calculated as a 3-D distance (Eqn. 2) between the nose of the first fish of the school to the caudal peduncle of the last fish in the school.

The values (3-D distance of the individuals, 3-D body angle, 3-D school length) calculated above were averaged among the three frames at each speed as a representative kinematic feature of the schools (or solitary fish) for each speed. The standard deviation of the angle to water flow in fish schools is calculated from the angular values of the individuals.

710 Tail beat frequency ($f_{TB}$), in Hz, is calculated as the number of tail beats observed within
711 one second. We sampled 10 tail beats from fish exhibiting steady-state swimming to obtain an
712 average and representative $f_{TB}$ for each solitary fish at each speed. We sampled 10 tail beats of
713 steady-state swimming for three individuals in the center of the fish school for an average and
714 representative $f_{TB}$ for each fish school.

715 Turning frequency is the total number of events when fish made a 90˚ turn in the 10-sec
716 video. To make the total number of turns per individual and fish schools comparable (multiple
717 individuals inevitably have a larger absolute number of turns), we derived the average turning
718 frequency per schooling fish by dividing the total number of turns of fish school by the number
719 of fish in the school.

720 Total energy expenditure per tail beat (kJ $kg^{-1}$ $beat^{-1}$) is calculated by TEE • ($f_{TB}$ • 60 $)^{-1}$ to
721 estimate the total metabolic energy spent to achieve one stride length.

722 Additional calculations of fluid dynamic metrics were:

723 Strouhal number = ($f_{TB}$ • tail beat amplitude) • $U^{-1}$ (*8*). Tail beat amplitude is measured as
724 the average distance of five peak-to-peak oscillation amplitudes of the tip of the fish's tail. The
725 measurement is conducted on the calibrated high-speed video in video analysis software
726 (Phontron FASTCAM Viewer 4, Photron USA, Inc.).

727 Reynolds number = (water density • $U$ • fish fork length) • water dynamic viscosity $^{-1}$ (*8*).
728 Water density and dynamic viscosity are given at 28 °C.

729

730 **Statistical analyses**

731 Measurement points are presented as mean ± s.e.m. For the metrics that failed normality
732 tests, logarithm transformations were applied to meet the assumptions of normality of residuals,
733 homoscedasticity of the residuals, and no trend in the explanatory variables. Since fish schools

exhibit the features of a coherent functional unit, the statistical model treated one school as one sample size, and the experiment measured five replicates of fish schools. The majority of statistical comparisons used the General Linear Model (Fixed factors: solitary fish vs. fish schools & swimming speeds, the label of solitary fish & fish schools as a random effect) with Holm–Šídák *post-hoc* tests. The few comparisons that used other statistical models are listed below. The comparison of $\dot{M}O_{2min}$ at $U_{opt}$, $\dot{M}O_2$ of aggregating behaviours exhibited at the lowest speed ($\dot{M}O_{2aggregate}$) and resting $\dot{M}O_2$ ($\dot{M}O_{2rest}$) in fish schools used one-way ANOVA with Holm–Šídák *post-hoc* tests. The comparison of EPOC between solitary fish and fish schools used a two-tailed Student's t-test. The comparison of the duration of EPOC between solitary fish and fish schools used a two-tailed Student's t-test. The overall difference in percentage aerobic scope (% aerobic scope) between fish schools and solitary individuals is compared by the Wilcoxon singed-rank test over the entire range of 14 swimming speeds. The statistical analyses were conducted in SPSS v.28 (SPSS Inc. Chicago, IL, USA). The best-fitting regression analyses were conducted using Prism v.9.4.1 (GraphPad Software, San Diego, CA, USA). 95% C.I. values were presented for all regression models as shaded areas around the regression or data points. Statistical significance is denoted by *, **, ***, **** for $p$-values of $\leq 0.05$, $\leq 0.01$, $\leq 0.001$, $\leq 0.0001$ respectively.

## References and Notes


1. A. Biewener, S. Patek, *Animal Locomotion* (Oxford University Press, 2018).

2. H. Weimerskirch, J. Martin, Y. Clerquin, P. Alexandre, S. Jiraskova, Energy saving in flight formation. *Nature* **413**, 697–698 (2001).

3. F. E. Fish, Kinematics of ducklings swimming in formation: Consequences of position. *Journal of Experimental Zoology* **273**, 1–11 (1995).

4. B. Blocken, T. van Druenen, Y. Toparlar, F. Malizia, P. Mannion, T. Andrianne, T. Marchal, G.-J. Maas, J. Diepens, Aerodynamic drag in cycling pelotons: New insights by CFD simulation and wind tunnel testing. *Journal of Wind Engineering and Industrial Aerodynamics* **179**, 319–337 (2018).

5. I. Shinichiro, Aerodynamic effects by marathon pacemakers on a main runner. *Transactions of the Japan Society of Mechanical Engineers Part B* **73**, 1975–1980 (2007).

6. D. Weihs, Hydromechanics of fish schooling. *Nature* **241**, 290–291 (1973).

7. Y. Zhang, G. V. Lauder, Energetics of collective movement in vertebrates. *Journal of Experimental Biology* **226**, jeb245617 (2023).

8. S. Vogel, *Life in Moving Fluids: The Physical Biology of Flow - Revised and Expanded Second Edition* (Princeton University Press, 1981).

9. J. Laforgia, R. T. Withers, C. J. Gore, Effects of exercise intensity and duration on the excess post-exercise oxygen consumption. *Journal of Sports Sciences* **24**, 1247–1264 (2006).

10. J. R. Brett, The respiratory metabolism and swimming performance of young sockeye salmon. *J. Fish. Res. Bd. Can.* **21**, 1183–1226 (1964).

11. F. W. H. Beamish, "Swimming capacity" in *Fish Physiology* (London: Academic Press, W.S. Hoar and D. J. Randall., 1978; https://cir.nii.ac.jp/crid/1571135650623593984)vol. VII, pp. 101–187.

12. S. J. Portugal, T. Y. Hubel, J. Fritz, S. Heese, D. Trobe, B. Voelkl, S. Hailes, A. M. Wilson, J. R. Usherwood, Upwash exploitation and downwash avoidance by flap phasing in ibis formation flight. *Nature* **505**, 399–402 (2014).

13. F. R. Parker Jr., Reduced metabolic rates in fishes as a result of induced schooling. *Transactions of the American Fisheries Society* **102**, 125–131 (1973).

14. M. V. Abrahams, P. W. Colgan, Risk of predation, hydrodynamic efficiency and their influence on school structure. *Environ Biol Fish* **13**, 195–202 (1985).

15. E. Burgerhout, C. Tudorache, S. A. Brittijn, A. P. Palstra, R. P. Dirks, G. E. E. J. M. van den Thillart, Schooling reduces energy consumption in swimming male European eels, Anguilla anguilla L. *Journal of Experimental Marine Biology and Ecology* **448**, 66–71 (2013).

16. M. Currier, J. Rouse, D. J. Coughlin, Group swimming behaviour and energetics in bluegill Lepomis macrochirus and rainbow trout Oncorhynchus mykiss. *Journal of Fish Biology* **98**, 1105–1111 (2021).

17. M. Hvas, F. Oppedal, Influence of experimental set-up and methodology for measurements of metabolic rates and critical swimming speed in Atlantic salmon Salmo salar. *Journal of Fish Biology* **95**, 893–902 (2019).

18. B. L. Partridge, T. J. Pitcher, Evidence against a hydrodynamic function for fish schools. *Nature* **279**, 418–419 (1979).

19. J. R. Usherwood, M. Stavrou, J. C. Lowe, K. Roskilly, A. M. Wilson, Flying in a flock comes at a cost in pigeons. *Nature* **474**, 494–497 (2011).

20. L. Li, M. Nagy, J. M. Graving, J. Bak-Coleman, G. Xie, I. D. Couzin, Vortex phase matching as a strategy for schooling in robots and in fish. *Nat Commun* **11**, 5408 (2020).

21. J. Kelly, Y. (潘宇) Pan, A. Menzer, H. (董海波) Dong, Hydrodynamics of body–body interactions in dense synchronous elongated fish schools. *Physics of Fluids* **35**, 041906 (2023).

22. F. E. Fish, C. M. Schreiber, K. W. Moored, G. Liu, H. Dong, H. Bart-Smith, Hydrodynamic performance of aquatic flapping: Efficiency of underwater flight in the Manta. *Aerospace* **3**, 20 (2016).

23. M. Kurt, K. W. Moored, Flow interactions of two- and three-dimensional networked bio-inspired control elements in an in-line arrangement. *Bioinspir. Biomim.* **13**, 045002 (2018).

24. K. D. Jones, C. M. Dohring, M. F. Platzer, Experimental and computational investigation of the Knoller-Betz effect. *AIAA Journal* **36**, 1240–1246 (1998).

25. J. D. Stewart, A. Barroso, R. H. Butler, R. J. Munns, Caught at the surface: myctophids make easy prey for dolphins and devil rays. *Ecology* **99**, 1894–1896 (2018).

26. T. J. Pitcher, A. E. Magurran, I. J. Winfield, Fish in larger shoals find food faster. *Behav Ecol Sociobiol* **10**, 149–151 (1982).

27. K. E. Jain, A. P. Farrell, Influence of seasonal temperature on the repeat swimming performance of rainbow trout Oncorhynchus mykiss. *Journal of Experimental Biology* **206**, 3569–3579 (2003).

28. P. E. Holder, C. M. Wood, M. J. Lawrence, T. D. Clark, C. D. Suski, J.-M. Weber, A. J. Danylchuk, S. J. Cooke, Are we any closer to understanding why fish can die after severe exercise? *Fish and Fisheries* **23**, 1400–1417 (2022).

29. O. A. Misund, A. Aglen, Swimming behaviour of fish schools in the North Sea during acoustic surveying and pelagic trawl sampling. *ICES Journal of Marine Science* **49**, 325–334 (1992).

30. S. J. Peake, A. P. Farrell, Fatigue is a behavioural response in respirometer-confined smallmouth bass. *Journal of Fish Biology* **68**, 1742–1755 (2006).

31. S. J. Peake, A. P. Farrell, Postexercise Physiology and Repeat Performance Behaviour of Free-Swimming Smallmouth Bass in an Experimental Raceway. *Physiological and Biochemical Zoology* **78**, 801–807 (2005).

32. Y. Zhang, M. J. H. Gilbert, A. P. Farrell, Finding the peak of dynamic oxygen uptake during fatiguing exercise in fish. *Journal of Experimental Biology* **222** (2019).

33. A. P. Farrell, S. M. Clutterham, On-line venous oxygen tensions in rainbow trout during graded exercise at two acclimation temperatures. *Journal of Experimental Biology* **206**, 487–496 (2003).

34. F. E. Fish, J. F. Fegely, C. J. Xanthopoulos, Burst-and-coast swimming in schooling fish (Notemigonus crysoleucas) with implications for energy economy. *Comparative Biochemistry and Physiology Part A: Physiology* **100**, 633–637 (1991).

35. G. A. Gaesser, G. A. Brooks, Metabolic bases of excess post-exercise oxygen consumption: a review. *Med Sci Sports Exerc* **16**, 29–43 (1984).

36. B. C. Jayne, G. V. Lauder, New data on axial locomotion in fishes: How speed affects diversity of kinematics and motor patterns. *American Zoologist* **36**, 642–655 (1996).

37. L. C. Rome, P. T. Loughna, G. Goldspink, Temperature Acclimation: Improved Sustained Swimming Performance in Carp at Low Temperatures. *Science* **228**, 194–196 (1985).

38. C. L. Milligan, Metabolic recovery from exhaustive exercise in rainbow trout. *Comparative Biochemistry and Physiology Part A: Physiology* **113**, 51–60 (1996).

39. M. Kjaer, J. Bangsbo, G. Lortie, H. Galbo, Hormonal response to exercise in humans: influence of hypoxia and physical training. *American Journal of Physiology-Regulatory, Integrative and Comparative Physiology* **254**, R197–R203 (1988).

40. H. F. Brown, D. Difrancesco, S. J. Noble, How does adrenaline accelerate the heart? *Nature* **280**, 235–236 (1979).

41. C. A. Ross, D. A. Ruggiero, D. H. Park, T. H. Joh, A. F. Sved, J. Fernandez-Pardal, J. M. Saavedra, D. J. Reis, Tonic vasomotor control by the rostral ventrolateral medulla: effect of electrical or chemical stimulation of the area containing C1 adrenaline neurons on arterial pressure, heart rate, and plasma catecholamines and vasopressin. *J. Neurosci.* **4**, 474–494 (1984).

42. Y. Zhang, G. Claireaux, H. Takle, S. M. Jørgensen, A. P. Farrell, A three-phase excess post-exercise oxygen consumption in Atlantic salmon Salmo salar and its response to exercise training. *Journal of Fish Biology* **92**, 1385–1403 (2018).

43. C. G. Lee, A. P. Farrell, A. Lotto, S. G. Hinch, M. C. Healey, Excess post-exercise oxygen consumption in adult sockeye (Oncorhynchus nerka) and coho (O. kisutch) salmon following critical speed swimming. *Journal of Experimental Biology* **206**, 3253–3260 (2003).

44. P. Webb PW;, Hydrodynamics and Energetics of Fish Propulsion. *Bulletin of the Fisheries Research Board of Canada* **Bulletin 190** (1975).

45. A. Costanzo, C. K. Hemelrijk, Spontaneous emergence of milling (vortex state) in a Vicsek-like model. *J. Phys. D: Appl. Phys.* **51**, 134004 (2018).

46. R. A. Rountree, Association of Fishes with Fish Aggregation Devices: Effects of Structure Size on Fish Abundance. *Bulletin of Marine Science* **44**, 960–972 (1989).

47. S. Camazine, J.-L. Deneubourg, N. R. Franks, J. Sneyd, G. Theraula, E. Bonabeau, *Self-Organization in Biological Systems* (Princeton University Press, 2020; https://www.degruyter.com/document/doi/10.1515/9780691212920/html).

48. S. Verma, G. Novati, P. Koumoutsakos, Efficient collective swimming by harnessing vortices through deep reinforcement learning. *Proceedings of the National Academy of Sciences* **115**, 5849–5854 (2018).

49. H. Ko, G. Lauder, R. Nagpal, The role of hydrodynamics in collective motions of fish schools and bioinspired underwater robots. *Journal of The Royal Society Interface* **20**, 20230357 (2023).

50. D. N. Beal, F. S. Hover, M. S. Triantafyllou, J. C. Liao, G. V. Lauder, Passive propulsion in vortex wakes. *Journal of Fluid Mechanics* **549**, 385–402 (2006).

51. J. C. Liao, D. N. Beal, G. V. Lauder, M. S. Triantafyllou, The Kármán gait: novel body kinematics of rainbow trout swimming in a vortex street. *J Exp Biol* **206**, 1059–1073 (2003).

52. D. Quinn, G. Lauder, Tunable stiffness in fish robotics: mechanisms and advantages. *Bioinspir. Biomim.* **17**, 011002 (2021).

53. G. V. Zuyev, V. V. Belyayev, An experimental study of the swimming of fish in groups as exemplified by the horsemackerel [Trachurus mediterraneus ponticus Aleev]. *Journal of ichthyology* **10**, 545–549 (1970).

54. S. Marras, S. S. Killen, J. Lindström, D. J. McKenzie, J. F. Steffensen, P. Domenici, Fish swimming in schools save energy regardless of their spatial position. *Behav Ecol Sociobiol* **69**, 219–226 (2015).

55. J. Herskin, J. F. Steffensen, Energy savings in sea bass swimming in a school: measurements of tail beat frequency and oxygen consumption at different swimming speeds. *Journal of Fish Biology* **53**, 366–376 (1998).

56. P. G. Bushnell, J. F. Steffensen, K. Johansen, Oxygen Consumption and Swimming Performance in Hypoxia-Acclimated Rainbow Trout Salmo Gairdneri. *Journal of Experimental Biology* **113**, 225–235 (1984).

57. C. Sepulveda, K. A. Dickson, Maximum Sustainable Speeds and Cost of Swimming in Juvenile Kawakawa Tuna (Euthynnus Affinis) and Chub Mackerel (Scomber Japonicus). *Journal of Experimental Biology* **203**, 3089–3101 (2000).

58. V. Di Santo, C. P. Kenaley, G. V. Lauder, High postural costs and anaerobic metabolism during swimming support the hypothesis of a U-shaped metabolism–speed curve in fishes. *Proceedings of the National Academy of Sciences* **114**, 13048–13053 (2017).

59. B. A. Block, D. Booth, F. G. Carey, Direct Measurement of Swimming Speeds and Depth of Blue Marlin. *Journal of Experimental Biology* **166**, 267–284 (1992).

60. B. A. Block, S. L. H. Teo, A. Walli, A. Boustany, M. J. W. Stokesbury, C. J. Farwell, K. C. Weng, H. Dewar, T. D. Williams, Electronic tagging and population structure of Atlantic bluefin tuna. *Nature* **434**, 1121–1127 (2005).

61. M. S. Triantafyllou, G. S. Triantafyllou, An Efficient Swimming Machine. *Scientific American* **272**, 64–70 (1995).

62. M. Kurt, J. Cochran-Carney, Q. Zhong, A. Mivehchi, D. B. Quinn, K. W. Moored, Swimming freely near the ground leads to flow-mediated equilibrium altitudes. *Journal of Fluid Mechanics* **875**, R1 (2019).

63. G. Timmerhaus, C. C. Lazado, N. A. R. Cabillon, B. K. M. Reiten, L.-H. Johansen, The optimum velocity for Atlantic salmon post-smolts in RAS is a compromise between muscle growth and fish welfare. *Aquaculture* **532**, 736076 (2021).

64. P. He, C. S. Wardle, Tilting behaviour of the Atlantic mackerel, Scomber scombrus, at low swimming speeds. *Journal of Fish Biology* **29**, 223–232 (1986).

65. K. Cathcart, S. Y. Shin, J. Milton, D. Ellerby, Field swimming performance of bluegill sunfish, Lepomis macrochirus: implications for field activity cost estimates and laboratory measures of swimming performance. *Ecology and Evolution* **7**, 8657–8666 (2017).

66. E. D. Gellman, T. R. Tandler, D. J. Ellerby, Swimming from coast to coast: a novel fixed-gear swimming gait in fish. *Biology Letters* **15**, 20190270 (2019).

67. N. W. Xu, J. O. Dabiri, Low-power microelectronics embedded in live jellyfish enhance propulsion. *Science Advances* **6**, eaaz3194 (2020).

68. K. Y. Lee, S.-J. Park, D. G. Matthews, S. L. Kim, C. A. Marquez, J. F. Zimmerman, H. A. M. Ardoña, A. G. Kleber, G. V. Lauder, K. K. Parker, An autonomously swimming biohybrid fish designed with human cardiac biophysics. *Science* **375**, 639–647 (2022).

69. M. B. S. Svendsen, P. G. Bushnell, J. F. Steffensen, Design and setup of intermittent-flow respirometry system for aquatic organisms. *Journal of Fish Biology* **88**, 26–50 (2016).

70. Y. Zhang, "Interpreting species, intraspecific and intra-individual variability by comprehensively characterizing a fish's respiratory phenotype with valid measures of oxygen uptake," thesis, University of British Columbia (2021).

71. R. J. Kline, D. C. Parkyn, D. J. Murie, Empirical Modelling of Solid-blocking Effect in a Blazka Respirometer for Gag, a Large Demersal Reef Fish. *Advances in Zoology and Botany* **3**, 193–202 (2015).

72. Y. Zhang, G. Claireaux, H. Takle, S. M. Jørgensen, A. P. Farrell, A three-phase excess post-exercise oxygen consumption in Atlantic salmon Salmo salar and its response to exercise training. *J Fish Biol* **92**, 1385–1403 (2018).

73. H. F. Wootton, J. R. Morrongiello, T. Schmitt, A. Audzijonyte, Smaller adult fish size in warmer water is not explained by elevated metabolism. *Ecology Letters* **25**, 1177–1188 (2022).

74. D. Chabot, J. F. Steffensen, A. P. Farrell, The determination of standard metabolic rate in fishes. *Journal of Fish Biology* **88**, 81–121 (2016).

75. J. C. Svendsen, C. Tudorache, A. D. Jordan, J. F. Steffensen, K. Aarestrup, P. Domenici, Partition of aerobic and anaerobic swimming costs related to gait transitions in a labriform swimmer. *Journal of Experimental Biology* **213**, 2177–2183 (2010).

76. A. E. Brafield, D. J. Solomon, Oxy-calorific coefficients for animals respiring nitrogenous substrates. *Comparative Biochemistry and Physiology Part A: Physiology* **43**, 837–841 (1972).

77. T. L. Hedrick, Software techniques for two- and three-dimensional kinematic measurements of biological and biomimetic systems. *Bioinspir. Biomim.* **3**, 034001 (2008).

78. M. Saadat, F. Berlinger, A. Sheshmani, R. Nagpal, G. V. Lauder, H. Haj-Hariri, Hydrodynamic advantages of in-line schooling. *Bioinspir Biomim* **16** (2021).

79. F. E. Fish, C. A. Hui, Dolphin swimming–a review. *Mammal Review* **21**, 181–195 (1991).

80. M. Daghooghi, I. Borazjani, The hydrodynamic advantages of synchronized swimming in a rectangular pattern. *Bioinspir. Biomim.* **10**, 056018 (2015).

**Acknowledgments:** Many thanks to members of Lauder Laboratory for numerous discussions about fish schooling behaviour, for comments on the manuscript, and to Cory Hahn for fish care.

**Funding:** Funding provided by the National Science Foundation grant 1830881 (GVL), the Office of Naval Research grants N00014-21-1-2661 (GVL), N00014-16-1-2515 (GVL), 00014-22-1-2616 (GVL), and a Postdoctoral Fellowship of Natural Sciences and Engineering Research Council of Canada PDF - 557785 – 2021 (YZ).

**Author contributions:**

Y.Z. and G.L. conceptualized the study. Y.Z. performed experiments and data analyses and wrote the manuscript. Y.Z. and G.L. provided manuscript edits and comments and approved the final version.

**Competing interests:** Authors declare that they have no competing interests.

**Data and materials availability:** All data generated or analysed during this study are included in this published article (and its supplementary information files).

**Supplementary Materials:**
Introductory text
Figs. S1 to S9
Tables S1 to S4

953 **TABLE HEADING**

954

955 **Table 1. A summary of experimental studies that directly estimate the energetic saving of**
956 **group movement in aerial and aquatic vertebrates that move through a fluid environment.**
957 No energetic measurements have made for freely-moving bird flocks. Three studies measured
958 the energetics of fish schools over a range of narrow speeds; two other studies measured the
959 energetics of fish schooling at one speed. But no studies have quantified *both* the aerobic and
960 anaerobic energetic cost of swimming as a group compared to solitary locomotion.

| Animal group | Species | Testing speeds | Group size | Measurements | Results | Reference |
|---|---|---|---|---|---|---|
| Bird | *Pelecanus onocrotalus* | Voluntary flights | < 8 | Heart rate | Group movement saves energy | Weimerskirch et al.,2001 |
| Bird | *Columba livia* | Voluntary flights | 6 | Flap frequency & Accelerations | Group movement costs more energy | Usherwood et al.,2011 |
| Bird | *Geronticus eremita* | Voluntary flights | 14 | Wing beat phase, spatial distribution | V-formation birds use phasing strategy to cope with wakes | Portugal et al., 2014 |
| Ray-finned fish | 15 species | 1 speed, unknown speed | 6–12 individuals | Aerobic energy | Grouping reduces metabolic rate | Parker, 1973 |
| Ray-finned fish | *Notropis heterodon* | 1 speed ~1.2 BL $s^{-1}$ | 3 individuals | Aerobic energy | Only schooling of 6 cm fish saves energy | Abrahams & Colgan, 1985* |
| Ray-finned fish | *Anguilla anguilla* L | 6 speeds 1-2.2 BL $s^{-1}$ | 7 individuals | Aerobic energy | Schooling save energy at low speeds | Burgerhout et al.,2013* |
| Ray-finned fish | *Lepomis macrochirus* *Oncorhynchus mykiss* | 4 speeds, 1.5-3 BL $s^{-1}$ | 1-8 individuals | Aerobic energy | Schooling saves energy | Currier et al., 2020* |
| Ray-finned fish | *Salmo salar* | 6 speeds 1-3 BL $s^{-1}$ | 10 individuals | Aerobic energy | Schooling does not save energy | Hvas & Oppedal, 2019 |
| Ray-finned fish | *Devario aequipinnatus* | 14 speeds, 0.3–8 BL $s^{-1}$ | 8 individuals | Aerobic & anaerobic energy | Schooling saves energy at high speed | Present study* |

*Studies used group and individual fish in the same size swim-tunnel respirometer

†Other uncited studies of fish schoolings use kinematic calculations and computer simulation to indirectly show that fish schooling conserve energy

## FIGURES & FIGURE CAPTIONS

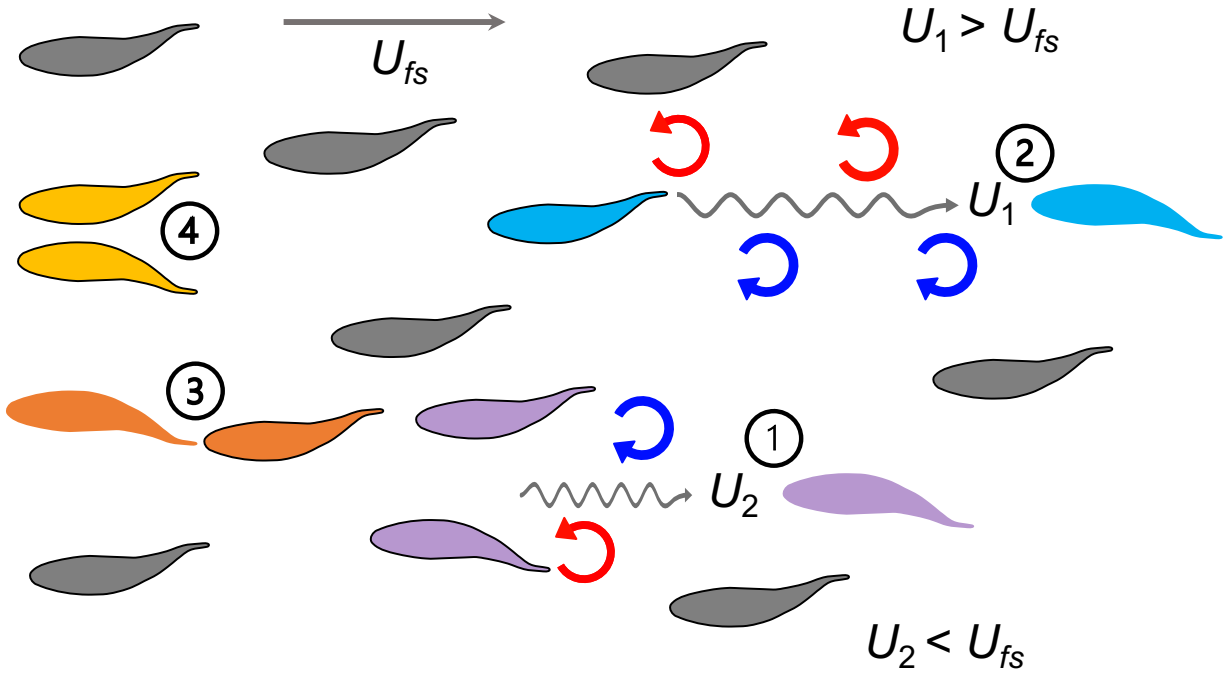


**Fig. 1. A summary of biomechanical principles underlying proposed hydrodynamic advantages of schooling behaviour in fish.** When fish swim into free-stream flow ($U_{fs}$), experimental data show that fish schools are dynamic with fish changing position frequently. Regardless of fish position within a school and changes in relative position, theoretical and robotic analyses have demonstrated that at least four mechanisms (indicated by numbers) provide an advantage in the form of reduced power consumption. 1. Reduced oncoming velocity ($U_2$) requires less thrust for a fish swimming in the wake between two leading fish (*6*); 2. The Knoller-Betz effect of leading edge suction reduces costs for a trailing fish due to accelerated oscillating flow at the head ($U_1$) (*24*) (*78*); 3. Added mass "push" from follower to leader can reduce costs for the leader in front of another fish (*79*) (*23*) (*78*); 4. Wall effects benefit neighbouring fish where swimming next to another fish reduces swimming costs (*80*) (*20*). These principles suggest that regardless of the relative positions of the individuals within the fish school, the fish school as a collective unit should be able to save metabolic energy compared to a solitary fish swimming in $U_{fs}$.

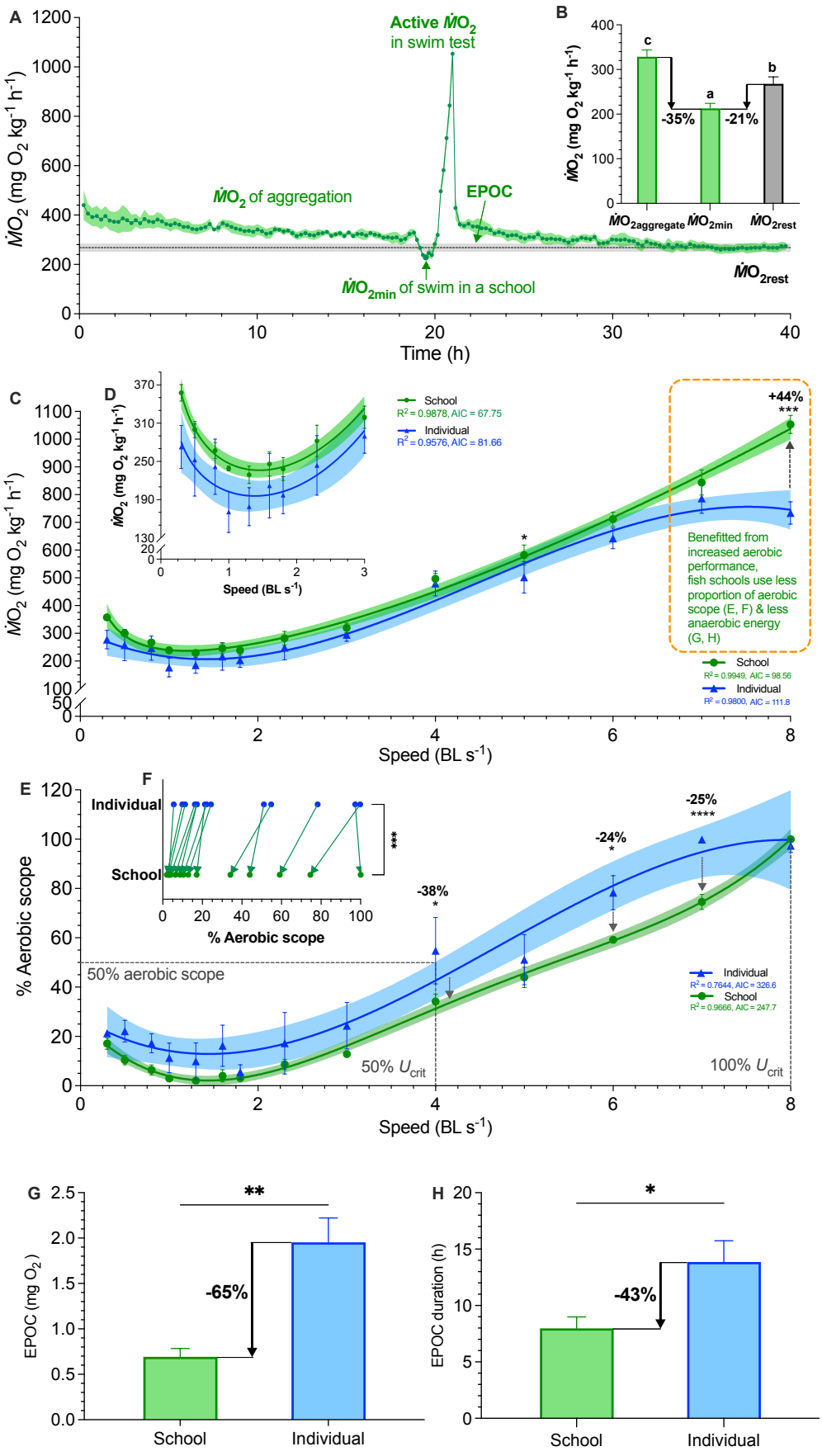
A
Active $\dot{M}O_2$ in swim test
$\dot{M}O_2$ of aggregation
EPOC
$\dot{M}O_{2min}$ of swim in a school
$\dot{M}O_{2rest}$
$\dot{M}O_2$ (mg $O_2$ kg$^{-1}$ h$^{-1}$)
Time (h)
B
c
a
b
-35%
-21%
$\dot{M}O_{2aggregate}$
$\dot{M}O_{2min}$
$\dot{M}O_{2rest}$
C
D
School
$R^2$ = 0.9878, AIC = 67.75
Individual
$R^2$ = 0.9576, AIC = 81.66
Speed (BL s$^{-1}$)
+44%
Benefitted from increased aerobic performance, fish schools use less proportion of aerobic scope (E, F) & less anaerobic energy (G, H)
School
$R^2$ = 0.9949, AIC = 98.56
Individual
$R^2$ = 0.9800, AIC = 111.8
E
F
Individual
School
% Aerobic scope
-38%
-24%
-25%
50% aerobic scope
50% $U_{crit}$
100% $U_{crit}$
Individual
$R^2$ = 0.7644, AIC = 326.6
School
$R^2$ = 0.9666, AIC = 247.7
G
EPOC (mg $O_2$)
-65%
School
Individual
H
EPOC duration (h)
-43%
School
Individual

983

984 **Fig. 2. Measurements of aerobic and anaerobic locomotor cost of fish schools and solitary**
985 **fish.** (**A**) Average traces of metabolic rate ($\dot{M}O_2$) of fish schools over a 40-hour experiment.
986 Following the first 18-h quiescent state, a critical swimming speed ($U_{crit}$) test quantifies the
987 aerobic cost of active swimming. The ensuing 18-h measurement of excess post-exercise oxygen
988 consumption (EPOC) quantifies the anaerobic cost. (**B**) Comparison of $\dot{M}O_2$ for conditions of
989 aggregating behaviour, minimum demand speed, and resting condition with minimal flow
990 ($\dot{M}O_{2aggregate}$, $\dot{M}O_{2min}$, $\dot{M}O_{2rest}$) (**C**) Comparisons of concave upward shaped $\dot{M}O_2$-speed curve
991 over the entire range (0.3–8 body length $s^{-1}$, BL $s^{-1}$) and (**D**) the concave shaped $\dot{M}O_2$-speed
992 curve at the lower speeds (0.3–3 BL $s^{-1}$). (**E, F)** Percentage (%) aerobic scope used by fish
993 schools and solitary fish during the $U_{crit}$ test. (**G**, **H**) Comparisons of EPOC and EPOC durations
994 between fish schools and solitary fish. Statistical significance is denoted by asterisk(s). Green
995 colour = school data (n=5 schools); blue colour = solitary fish data (n=5 individual fish); shading
996 indicates the 95% confidence interval. Statistical details are available in the statistical analyses
997 section.

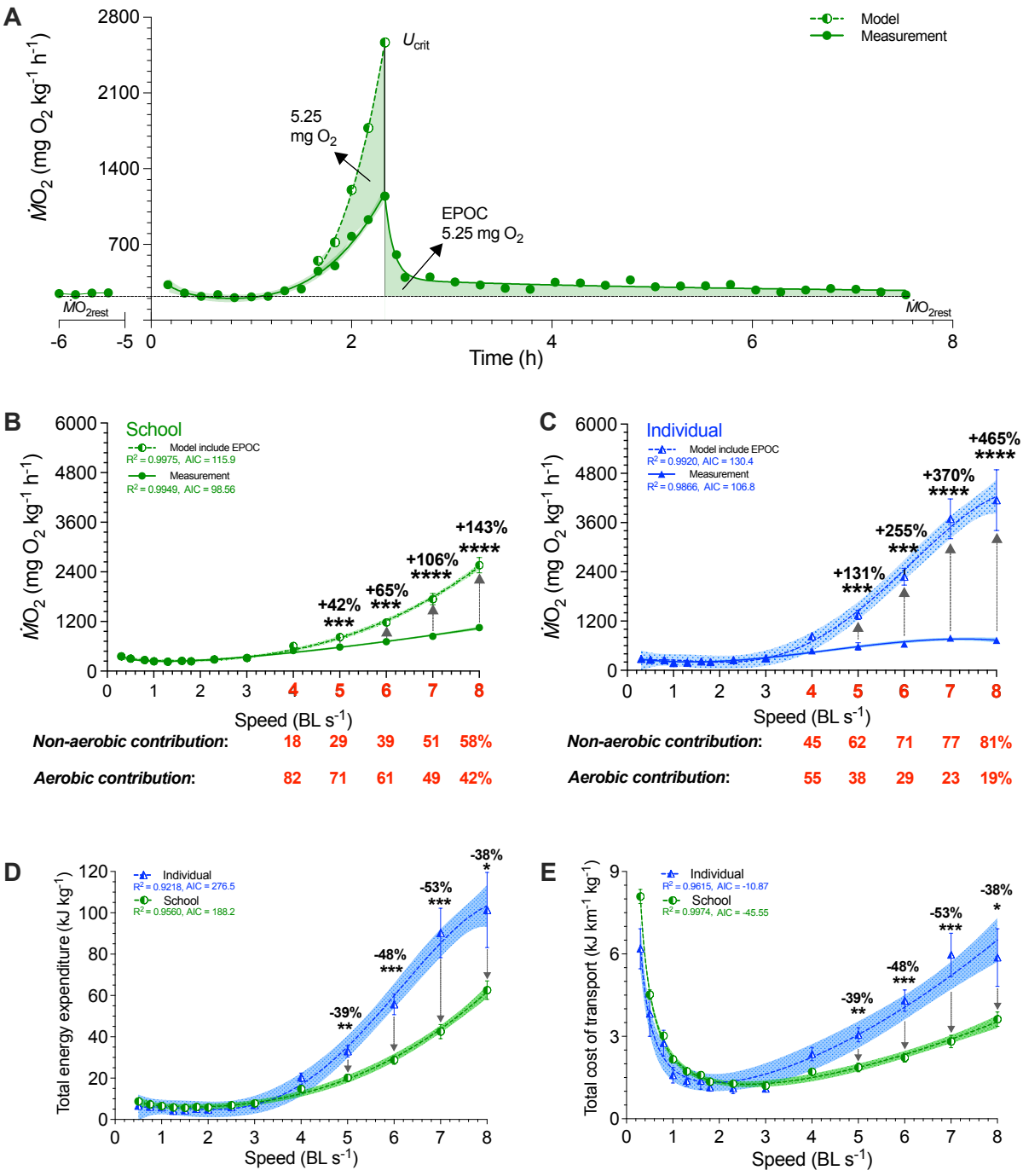
A
Model
Measurement
$U_{crit}$
5.25 mg $O_2$
EPOC 5.25 mg $O_2$
$\dot{M}O_2$ (mg $O_2$ kg$^{-1}$ h$^{-1}$)
$\dot{M}O_{2rest}$
Time (h)
B
School
Model include EPOC
$R^2$ = 0.9975, AIC = 115.9
Measurement
$R^2$ = 0.9949, AIC = 98.56
+42% ***
+65% ***
+106% ****
+143% ****
Speed (BL s$^{-1}$)
Non-aerobic contribution: 18 29 39 51 58%
Aerobic contribution: 82 71 61 49 42%
C
Individual
Model include EPOC
$R^2$ = 0.9920, AIC = 130.4
Measurement
$R^2$ = 0.9866, AIC = 106.8
+131% ***
+255% ***
+370% ****
+465% ****
Non-aerobic contribution: 45 62 71 77 81%
Aerobic contribution: 55 38 29 23 19%
D
Individual
$R^2$ = 0.9218, AIC = 276.5
School
$R^2$ = 0.9560, AIC = 188.2
-39% **
-48% ***
-53% ***
-38% *
Total energy expenditure (kJ kg$^{-1}$)
E
Individual
$R^2$ = 0.9615, AIC = -10.87
School
$R^2$ = 0.9974, AIC = -45.55
-39% **
-48% ***
-53% ***
-38% *
Total cost of transport (kJ km$^{-1}$ kg$^{-1}$)

998

**Fig. 3. Modeling of simultaneous aerobic and non-aerobic costs of fish schools and solitary fish for a critical swimming speed ($U_{crit}$) test. (A)** Modeling the $O_2$ cost of the metabolic rate ($\dot{M}O_2$)-speed curve and the ensuing recovery cost (excess post-exercise oxygen consumption, EPOC) as a function of speed. After $U_{crit}$, fish returned to the same resting $\dot{M}O_2$ ($\dot{M}O_{2rest}$) as a pre-test. (**B, C**) In addition to $\dot{M}O_2$ (solid line & filled symbols), we modeled the total $O_2$ cost (dash line & half-filled symbols) for fish schools and solitary fish and when performing the $U_{crit}$ swimming test. The estimated partitioning of aerobic and non-aerobic contributions to swimming are denoted (red-&-bold) with respect to speed for 4–8 BL $s^{-1}$ is shown below each graph. (**D, E**) Using total $O_2$ cost, we computed total energy expenditure (10-min period per point) and the total cost of transport (including both aerobic metabolism, high-energy phosphate, and anaerobic glycolysis) for both fish schools and solitary fish. Statistical significance is denoted by asterisk(s). Green colour = school data (n=5); blue colour = solitary fish data (n=5); shading indicates the 95% confidence interval. See methods for modeling and statistical details.

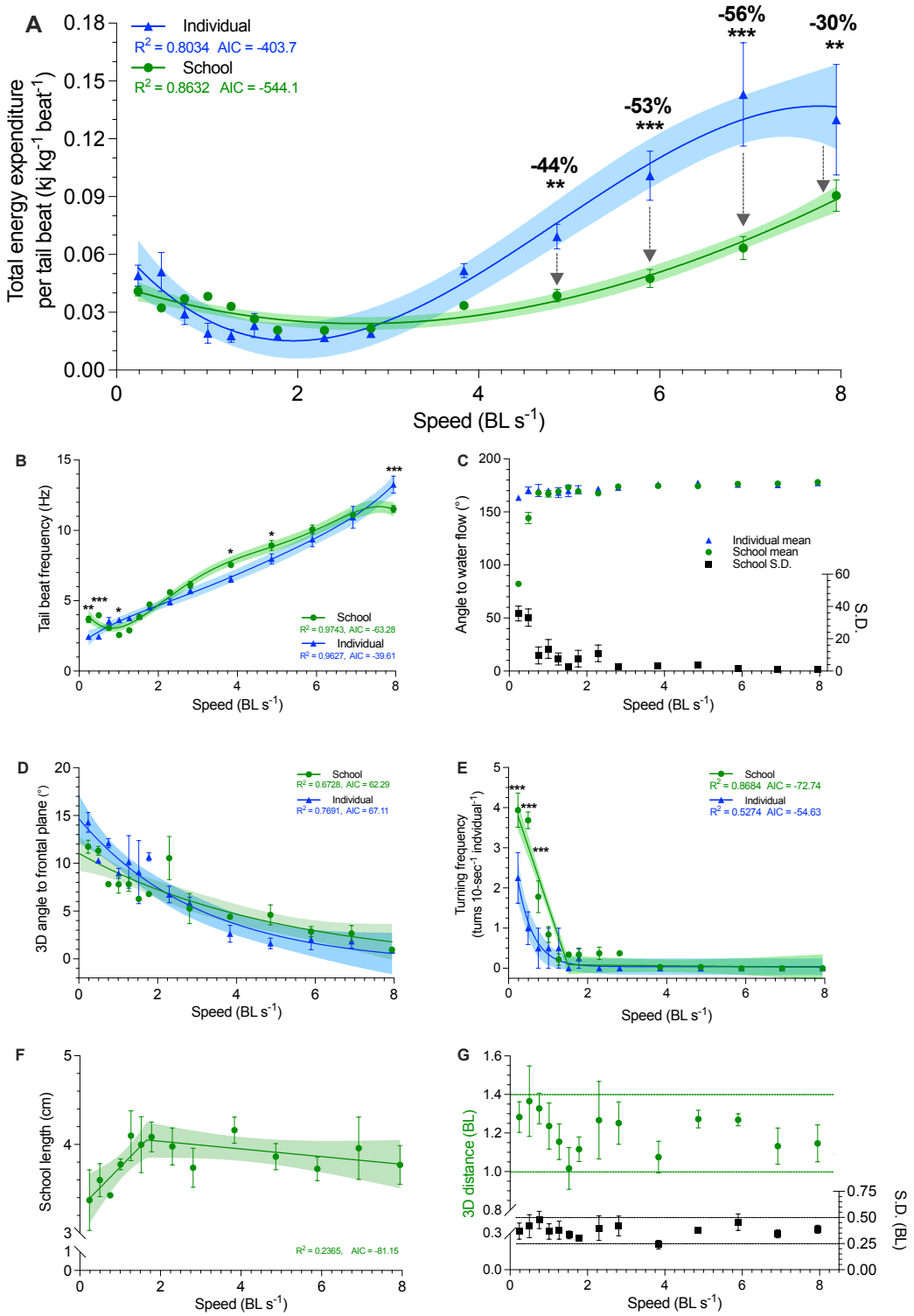
A
Individual
R2 = 0.8034 AIC = -403.7
School
R2 = 0.8632 AIC = -544.1
Total energy expenditure per tail beat (kj kg-1 beat-1)
Speed (BL s-1)
-44% **
-53% ***
-56% ***
-30% **
B
Tail beat frequency (Hz)
School
R2 = 0.9743, AIC = -63.28
Individual
R2 = 0.9627, AIC = -39.61
C
Angle to water flow (°)
S.D.
Individual mean
School mean
School S.D.
D
3D angle to frontal plane (°)
School
R2 = 0.6728, AIC = 62.29
Individual
R2 = 0.7691, AIC = 67.11
E
Turning frequency (turns 10-sec-1 individual-1)
School
R2 = 0.8684 AIC = -72.74
Individual
R2 = 0.5274 AIC = -54.63
F
School length (cm)
R2 = 0.2365, AIC = -81.15
G
3D distance (BL)
S.D. (BL)

1012

1013 **Fig. 4. Three-dimensional characterization of swimming kinematics and fish schooling**
1014 **dynamics as a function of speed. (A)** Total energy expenditure (TEE) per tail beat, (**B**) Tail beat
1015 frequency, (**C**) The angle of fish to free-stream water flow, measured as the mean and the S.D. of
1016 the angles of the individuals within the school. (**D**) Three-dimensional angle of fish to the frontal
1017 plane. (**E**) Turning frequency, (**F**) Three-dimensional school length. (**G**) Three-dimensional
1018 distances among all individuals in the school and the S.D. of the distance. The upper and lower
1019 boundaries of the metrics are indicated. Statistical significance is denoted by asterisk(s). Green
1020 colour = school data (n=3-4); blue colour = solitary fish data (n=3-4); shading indicates the 95%
1021 confidence interval. See methods for details of three-dimensional reconstruction and statistics.